2.4S.4 Potential Dam Failures

The following site-specific supplement addresses COL License Information Items 2.14 and 3.5.

This section addresses the SRP Section 2.4.4 Acceptance Criteria Limits from the reference Table 2.1-1, which states that the flood level from failure of existing and potential upstream or downstream water control structures will not exceed 30.5 cm (1.0 ft) below grade. The nominal plant grade for the safety facilities of STP 3 & 4 is 34.0 ft mean sea level (MSL) and the design entrance level slab elevation is 35.0 ft MSL. The design basis flood level at STP 3 & 4 based on the worst case dam failure scenario, the postulated MCR embankment breach, was conservatively established as 40.0 ft MSL, exceeding the reference ABWR DCD site parameter flood level criteria. The departure from the DCD site parameter flood level and the evaluation summary are documented in STP DEP T1 5.0-1. Subsection 2.4S.4 develops the flooding design basis for considering potential hazards to the safety-related facilities due to potential dam failures.

The STP 3 & 4 site is located on the west bank of the Colorado River in Matagorda County, Texas, about 10.5 river miles upstream of the Gulf Intracoastal Waterway (GIWW). There are a total of 68 dams with storage capacity in excess of 5000 acre-feet (AF) on the Colorado River and its tributaries upstream of the STP site. These dams and reservoirs are owned and operated by different entities including the Lower Colorado River Authority (LCRA), the U.S. Bureau of Reclamation (USBR), the Colorado River Municipal Water District (CRMWD), other local municipalities and utilities. Figures 2.4S.4-1(a) and 2.4S.4-1(b) show the locations of the 68 dams. Specific information of these dams that are relevant to the flood risk assessment of STP 3 & 4 is summarized in Table 2.4S.4-1, based on data collected primarily from the Texas Water Development Board (TWDB), Texas Commission for Environmental Quality (TCEQ), and LCRA. The six hydroelectric dams – Buchanan, Roy Inks, Alvin Wirtz, Max Starcke, Mansfield, and Tom Miller, owned and operated by LCRA are known as the Highland Lake dams.

In Texas, both private and public dams are monitored and regulated by TCEQ under the Dam Safety Program. Existing dams, as defined in Rule §299.1 Title 30 of the Texas Administrative Code (Reference 2.4S.4-1), are subject to periodic re-evaluation in consideration of continuing downstream development. Hydrologic criteria contained in Rule §299.14 of Title 30 (Table 3) on Hydrologic Criteria for Dams are the minimum acceptable spillway evaluation flood (SEF) for re-evaluating dam and spillway capacity for existing dams to determine whether upgrading is required. Similarly, on the structural considerations, evaluation of an existing dam includes, but is not limited to, visual inspections and evaluations of potential problems such as seepage, cracks, slides, conduit and control malfunctions, and other structural and maintenance deficiencies which could lead to failure of a structure.

Following the 1987 National Dam Safety Inspection Program recommendations of the Texas Water Commission, a predecessor agency of the TCEQ, to upgrade two of the Highland Lake dams due to unsafe condition, LCRA initiated a program to evaluate all six Highland Lake dams with respect to hydrologic, structural and geotechnical criteria.

In 1990, LCRA began a 15-year plan of Dam Modernization Program to address the safety condition of five of the six dams. A 1992 dam safety evaluation study commissioned by LCRA (Reference 2.4S.4-2) indicates that Wirtz, Starcke, and Tom Miller Dams would be overtopped during a Probable Maximum Flood (PMF) event, and certain sections of Buchanan, Wirtz, and Tom Miller Dams could have instability problems during severe flood conditions. The concrete dam sections of Mansfield Dam, however, would be stable during the PMF. At the completion of LCRA's Dam Modernization Program in January of 2005, substantial upgrade work had been undertaken at Buchanan, Inks, Wirtz, and Tom Miller Dams to address the unsafe conditions (Reference 2.4S.4-3). Upgrade at Mansfield Dam was considered not necessary as it is able to withstand the PMF without further reinforcement. Even in the event of failures of either Buchanan, Inks, Wirtz, or Starcke dams, Mansfield Dam would hold their flood volumes without overtopping (Reference 2.4S.4-4).

The UFSAR of STP 1 & 2 (Reference 2.4S.4-5) identifies two dam failure scenarios that are most critical to the flooding at the STP site. They are: (1) the breaching of the embankment of the onsite Main Cooling Reservoir (MCR); and (2) the postulated cascade failure of the major upstream dams on the Colorado River. These two scenarios also form the basis of the maximum flood level evaluation for STP 3 & 4 resulting from potential dam failures because the watershed and topographic conditions remain relatively unchanged since the preparation of the UFSAR for STP 1 & 2, and also because there are no new dams (including the previously proposed Columbus Bend Dam) planned for the Colorado River in the next 50 years, according to the 2007 State Water Plan (Reference 2.4S.3-6, also discussed in Subsection 2.4S.3.4.2) The dam failure scenarios and the postulated flood risk are discussed further in the following subsections.

2.4S.4.1 Dam Failure Permutations

2.4S.4.1.1 Failures of Upstream Dams on the Colorado River

Of all the dams on the Colorado River upstream of the STP 3 & 4 site, Mansfield Dam would generate the most significant dam break flood risk on the site. Mansfield Dam has the largest dam height of 266.4 ft and the largest reservoir storage capacity of 3.3 million acre-feet (MAF), at top of the dam. Among all the dams upstream, Mansfield Dam is also closest to the site at about 305 river miles upstream of the STP 3 & 4 site. The next major dam upstream that could pose significant flood risk to the site is the Buchanan Dam located at about 402 river miles upstream of STP 3 & 4. It has a height of 145.5 ft and a top-of-dam storage capacity of 1.18 MAF. Further upstream, the Simon Freese Dam, with a height of 148 ft and a top-of-dam storage capacity of 1.47 MAF, and the Twin Buttes Dam, with a height of 134 ft and top-of-dam storage capacity of 1.29 MAF are considered to have major, though not as significant, contribution to the flood risk at the STP site. They are located at about 199 miles and 290 miles, respectively, upstream of Buchanan Dam.

There are two failure permutations postulated of the upstream dams:

■   Scenario No. 1 – Simultaneous failure of all upstream dams induced by a seismic event. The failure is to occur coincidentally with a 2-year design wind event and a

500-year flood or a one-half probable maximum flood (PMF) per American National Standard ANSI/ANS-2.8 (Reference 2.4S.4-7).

- Scenario No. 2 – Domino-type failure of upstream dams with the same coincidental wind and flood events as in Scenario No. 1. It is postulated that the upstream-most dam(s) would fail first, thereby releasing a dam break flood wave (or waves) that propagates downstream and triggers the failure of the downstream dams one after another in a cascading manner. It is assumed that the 56 dams on the Colorado River and its tributaries upstream of Buchanan Dam (with top-of-dam capacity over 5000 AF) would fail in such a manner that their flood flow, expressed in terms of their respective top-of-dam storage volumes, would arrive at Lake Buchanan at approximately the same time, triggering the failure of Buchanan Dam. The dam break flood flow from Buchanan Dam would then propagate downstream to Lake Travis, overtopping Mansfield Dam and causing it to fail. The dam break flood from Mansfield Dam then propagates downstream to the STP 3 & 4 site. The failure is to occur coincidentally with a 2-year design wind event and a 500-year flood or a one-half probable maximum flood (PMF) per American National Standard ANSI/ANS-2.8 (Reference 2.4S.4-7).

Three upstream dams, Inks, Wirtz, and Starcke, located between Buchanan and Mansfield Dams, and two other upstream dams, Tom Miller and Longhorn Dams, located at 20 miles and 27 miles downstream of Mansfield Dam, were not included in the dam break analysis as their dam heights and potential flood volumes would have insignificant impact on the flood risk as compared to Mansfield Dam or Buchanan Dam.

There are five "off-channel" dams located on the tributaries of the Colorado River between Mansfield Dam and the STP site. They are: Decker Creek Dam (Lake Long), Bastrop Dam, Cummins Creek WS SCS Site 1 Dam, Cedar Creek Dam (Fayette Reservoir), and Eagle Lake Dam. These off-channel storage dams were also assumed to have no effect on the maximum dam break flood level at the STP 3 & 4 site, as compared to the major dams on the main stem of the Colorado River.

Of these two permutations, Scenario No. 2 would generate the most critical flood level at STP 3 & 4 because of the deliberate alignment of the travel and arrival of the dam breach flood volumes and flood peaks from the major upstream dams. Consequently, only the flood risk resulting from Scenario No. 2 was further evaluated.

Upstream dam failures induced by hydrologic causes such as probable maximum flood (PMF) will not be the controlling scenario in the evaluation of the maximum flood risk at the STP site. This is because the large dams with high hazard potential, such as O.C. Fischer, Simon Freese, Buchanan and Mansfield Dams, as listed in Table 2.4S.1-1, were either designed or have been upgraded to accommodate and sustain their respective PMFs in accordance with the hydrologic criteria for dams as defined in Rule 299.14 Title 30 of the Texas Administrative Code (Reference 2.4S.4-1). Mansfield Dam, in particular, would be able to hold the dam break flood volumes of either Buchanan, Wirtz, or Starcke Dams. Besides, the assumption that a domino-type dam failure of the 56 dams upstream of Buchanan with an aggregated top-of-dam storage volume of 6.87 MAF all arriving at Buchanan at about the same time is highly

conservative and would have bounded the potential flood risk caused by hydrological dam failures.

2.4S.4.1.2 Postulated Failure of the Main Cooling Reservoir

The MCR is enclosed by a rolled-earthen embankment, rising an average of 40 ft above the natural ground surface south of the plant site. The interior reservoir side slopes of the MCR embankment are lined with 2 feet thick soil cement. The centerline of the north embankment is approximately 2340 ft south of the centerline of the reactor buildings of STP 3 & 4. Site grade near the northern embankment is in the range of El. 27 ft MSL to El. 29 ft MSL, and the top of the embankment is at about El. 65.75 ft MSL. Normal maximum operating level of the reservoir is at El. 49.0 ft MSL, which is about 20 to 22 ft higher than the site grade near the northern embankment. Postulated failure mechanisms of the earth embankment include excessive seepage from piping through the foundations of the embankment, seismic activity leading to potential liquefaction of the foundation soils, and erosion of the embankment due to overtopping from flood or wind-wave events.

As discussed in the STP 1 & 2 UFSAR (Reference 2.4S.4-5), failure of the MCR embankment due to any of these probable mechanisms is not considered a credible event. Nevertheless, it is conceivable that a failure of the internal drainage system within the MCR embankment could saturate the embankment and allow seepage through it, which could then initiate a piping failure. Therefore, a piping failure of the MCR embankment was investigated and analyzed.

The northern MCR embankment, near the proposed circulating water intake and discharge pipeline, is the most critical location for piping failure because it is closest to, and inline with, Units 3 and 4. Two breach locations were considered for the analysis, one immediately east and one immediately west of the circulating water pipeline. Further discussion of breach parameter selection is presented in Subsection 2.4S.4.2.2.2.2.

2.4S.4.1.3 Potential for Landslide and Waterborne Missiles

The potential for major scale landslide, and hence blockage of streams on the Lower Colorado River in the vicinity of the STP site, is highly improbable due to the flat terrain. This is consistent with the conclusion of the UFSAR for STP 1 & 2 (Reference 2.4S.4-5). According to the investigation, there is no threat posed to the STP site due to surge from bank material sliding into the Lower Colorado River.

The potential for waterborne missiles reaching the STP site due to upstream dam failure is not considered to be critical because the site is located in the flood plain of the Lower Colorado River where the flood flow velocities are in general substantially lower than that in the main channel. Although there is a potential for waterborne missiles due to the MCR embankment breach, these missiles are not considered to be critical to the design of the safety related structures compared to tornado missiles. The static and dynamic effects of the MCR embankment breach on the plant structures are discussed in Section 3.4.

2.4S.4.2 Unsteady Flow Analysis of Potential Dam Failures

2.4S.4.2.1 Colorado River Dams

The dams on the Colorado River are discussed in Subsection 2.4S.4.1. Table 2.4S.4-1 lists the height, length, top-of-dam storage capacity, type, and year of completion of the 68 dams with a top-of-dam storage capacity larger than 5000 AF each. Of these 68 dams, Mansfield Dam, Buchanan Dam and 56 other dams upstream of Buchanan Dam were selected for inclusion in the dam break analysis. Dams with less than 5000 AF storage capacity, i.e., less than 0.2% of that of Mansfield Dam, were excluded from further evaluation as the impact of their potential breaching on the flood risk at the site would be minimal. The top-of-dam storage volume of Mansfield Dam is about 3.3 MAF, estimated from the elevation-storage capacity curves given in Reference 2.4S.4-8. Similarly, the top-of-dam storage volume of Buchanan Dam is estimated to be about 1.18 MAF. The combined top-of-dam-storage volume of the 56 dams upstream of Buchanan Dam is 6.87 MAF.

2.4S.4.2.1.1 Conceptual Unsteady Flow Analytical Model

The dam breach option of the USACE River Analysis System computer program (HEC-RAS) Version 3.1.3 (Reference 2.4S.4-9) was used to simulate the dam breach flood waves, which were then routed downstream to the STP 3 & 4, using the unsteady flow option of the program.

In the conceptual dam break flood model, the 56 dams upstream of Buchanan Dam would fail in a domino manner, with their combined top-of-dam storage capacity, totaling 6.87 MAF, arriving at Buchanan Dam at approximately the same time. As the flood level at Buchanan Dam rises to about 3 ft over the dam crest elevation of 1025.35 ft MSL, the dam would fail, thereby releasing the flood storage of Buchanan Dam plus the combined flood volumes from the 56 upstream dams. In accordance with the combined events requirements stipulated in the American National Standard ANSI/ANS-2.8 (Reference 2.4S.4-7), the evaluation of potential flood risks as a result of non-hydrologic dam break failures should also consider a coincidental event equal to a 500-year flood or one-half probable maximum flood (PMF), whichever is less. In this analysis, a constant flood flow of 500,000 cfs, slightly higher than the peak Standard Project Flood (SPF) inflow at Buchanan Dam and the 500-year flood peak inflow at Mansfield Dam, was conservatively used to represent the coincidental flow. The SPF and 500-year flood flow at several locations on the Colorado River are listed in Table 2.4S.4-2. They were estimated by Halff Associates, Inc. as part of the Lower Colorado River flood damage evaluation project conducted for LCRA and Fort Worth District Army Corps of Engineer (Reference 2.4S.4-10). The 500,000 cfs coincidental flow was applied to the entire model reach from Buchanan Dam to the downstream boundary at 4600 ft (0.9 river miles) upstream of the Gulf Intracoastal Waterway.

The flood wave from the breaching of Buchanan Dam would propagate down to the 266.4-ft high Mansfield Dam, with a crest elevation at 754.1 ft MSL and a top-of-dam storage capacity of 3.30 MAF. (In 1941, a 4-ft parapet wall was added to the dam crest raising its elevation from 750.1 ft MSL to 754.1 ft MSL to provide additional flood storage capacity.) Mansfield Dam was postulated to fail when it was overtopped by 3

ft at El. 757.1 ft MSL. The three dams located between Buchanan and Mansfield Dams: Roy Inks, Alvin Wirtz, and Max Starcke Dams, have a combined storage of about 298,300 AF. These dams were not assumed to fail in the dam break model because their combined total storage amounts to only about 9% of the total dam break flood volume at Mansfield. The SPF flood hydrographs from 19 tributaries between Buchanan and Mansfield Dams as estimated by Halff Associates, Inc. in the flood damage evaluation study (Reference 2.4S.4-10) were included as tributary inflows to this reach. The tributary inflows together with the dam break flood wave from Mansfield Dam were then routed to the STP 3 & 4 site in the HEC-RAS model.

2.4S.4.2.1.2 Physical Dam Data and Estimates of Breached Sections

Buchanan Dam, located at about 402 river miles upstream of STP 3 & 4, is 10,987 ft in length. It has two separate multiple concrete arch sections as well as a number of gravity sections (Reference 2.4S.4-8). The main dam section consists of 29 concrete arches, each of 70 ft in width and 145.5 ft in height. The total length of this multiple concrete arch section is 2030 ft and it occupies the deepest part of the river channel. To the right (looking downstream) is another shorter multiple concrete arch section of 805 ft in length, consisting of 23 arches of 35 ft wide each. Following the guidelines from Federal Energy Regulatory Commission (FERC) on dam break analysis (Reference 2.4S.4-11), 15 of the 29 larger arches (70 ft wide each) and 12 of the 23 smaller arches (35 ft wide each) were assumed to breach in the simulation. The breach section in the model was represented by a vertical section with a total width of 1470 ft and extending from the top of the dam to the bottom. The time to complete the breach was assumed to be 0.1 hour, based on the guidelines from FERC for the estimation of the dam breach parameter (Reference 2.4S.4-11). The model cross-section at Buchanan Dam is shown in Figure 2.4S.4-2.

Mansfield Dam, at about 305 river miles upstream of STP 3 & 4, has a 2710 ft long, 266.4 ft high concrete gravity section occupying the main river channel, and a 4380 ft long earthen rockfill saddle section with a maximum height of about 150 ft on the left side (looking downstream) (Reference 2.4S.4-8). The total storage capacity is 3.13 MAF at the dam crest elevation of 750.1 ft MSL. With the installation of the 4-ft parapet wall in 1941, the storage capacity increased to 3.30 MAF. Following the FERC guidelines (Reference 2.4S.4-11), about half of the 2710 ft concrete gravity section was postulated to fail when overtopped by 3 ft, resulting in a 1360 ft wide vertical breached section from top to bottom. The time to complete the breach was also assumed to be 0.1 hour. The model cross-section for Mansfield Dam is shown in Figure 2.4S.4-3.

Table 2.4S.4-3 lists the dam breach characteristics used to model the failure of these two dams.

2.4S.4.2.1.3 Channel Geometry

The channel geometry in the HEC-RAS dam break model was adopted from the river cross-sectional data of Halff's flood damage evaluation study for the Lower Colorado River (Reference 2.4S.4-10 and discussed in Subsection 2.4S.4.3). The Halff model has a total model reach length of 474 river miles represented by 1048 cross-sections

from Texas Highway 190 upstream of Buchanan Dam, to a section at 4600 ft (0.9 river miles) upstream of the Gulf Intracoastal Waterway just north of Matagorda Bay. The HEC-RAS dam break model developed for STP 3 & 4 has a shorter river reach of 414 miles starting from Buchanan Dam on the upstream end and was represented by a total of 793 model cross-sections. All bridge crossings specified in the Halff model were removed because they were assumed to be washed away during the dam break event. In addition, all ineffective flow areas as well as levees specified in the Halff model were also removed, when deemed appropriate. The locations of these cross-sections are shown in Figure 2.4S.4-4. The elevations of each of the cross-sections were referenced to the North America Vertical Datum 1988 (NAVD 88) in the Halff study. The HEC-RAS dam break model runs were also conducted in NAVD 88 datum. However, the flood level predictions were converted to MSL (or NGVD 29) for comparison with the STP plant grades.

Because the top-of-dam storage at Buchanan Dam was estimated to be 1.18 MAF, while the aggregated total top-of-dam storage of the 56 selected dams upstream of Buchanan Dam was estimated to be 6.87 MAF, it would not be possible for Buchanan Dam to accommodate the entire dam break flood volume from the breaching of these upstream dams. In order to properly account for the residual flows that could still arrive at and propagate downstream of Buchanan Dam after its failure, new model cross sections were introduced upstream of Buchanan Dam to extend the model reach by 36 miles to approximate the additional volume required to accommodate the combined dam break flood flow of 6.87 MAF from the dams upstream. The upstream reach extension consists of 37 rectangular cross sections 16,030-ft wide with a bottom elevation at 915.8 ft MSL. The cross-sectional width of 16,030 ft is similar to those of the three cross-sections behind Buchanan Dam in the Halff model (Reference 2.4S.4-10). The total flood volume in the model simulation would be over 8.0 MAF behind Buchanan Dam when it breaches at 3 ft above dam crest.

The primary objectives of the Halff study are for flood damage evaluations of the Lower Colorado River and therefore the model predictions were conducted for flood events up to the SPF. During extreme floods, inter-basin spillage could occur. Flood flow from the Colorado River could overspill into its neighboring sub-basins, such as Tres Palacios River to the west and San Bernard River and Peyton Creek to the east. In the flood of 1913, floodwaters from the Colorado River sub-basin overflowed into Caney Creek sub-basin to the east of the Colorado River near Wharton. With predictably higher flood discharges during the postulated dam failure scenario, the channel cross sections of the Halff study need to be extended beyond their limits to more accurately reflect the additional floodplain areas that would be inundated during the passage of the dam break flood waves. As HEC-RAS would automatically assume a vertical wall at the pre-set boundaries of the flood channel or floodplain, the extension could mitigate potentially unrealistic flood levels as a result of artificial limitation on the cross-sectional geometries imposed by the model setup. This can have a significant impact on the predicted flood peak in the lower reach of the river near the STP 3 & 4 site, where the drainage divides between sub-basins are relatively low in elevation.

A comparison was made between the simulated water levels from the initial dam break runs and the elevations of the drainage divides to determine the approximate location

where inter-basin spillage would occur. It was found that inter-basin spillage could occur near Garwood. Therefore, about 1.9-mile extension was added to the Halff model cross sections on each side starting from near Garwood. The width of the extension on each side was gradually increased to about 9.5 miles near Wharton down the river. Because the topography is, in general, higher west of the Colorado River towards the Palacio River sub-basin, the cross-sectional extensions in the downstream reach shifted eastward towards the San Bernard River and the Peyton Creek sub-basins. Eventually, near the STP 3 & 4 site, the river cross-sections were extended towards the east for some 17 miles. Typical model cross-sections at four locations on the model river reach including the extended sections are shown in Figures 2.4S.4-5 to 2.4S.4-8.

The USGS 30-m National Elevation Dataset (NED) digital elevation model data used to establish the cross-sectional extensions was referenced to MSL (or NGVD 1929), while the Halff model was referenced to NAVD 88. As the difference between these two datum references for this reach of the Lower Colorado River is less than 0.3 ft, no corrections to the datum, except for 32 sections, were made to adjust the elevations of the extensions to NAVD 88 datum. The 32 sections with datum corrected were located between the STP site and the downstream boundary and were adopted from the PMF routing model described in Subsection 2.4S.3.

The locations and extents of the cross-sections used in the HEC-RAS dam break model are shown in Figure 2.4S.4-4.

2.4S.4.2.1.4 Manning's *n* Values Used in the HEC-RAS Model

The Manning's *n* values used in the Halff HEC-RAS model were calibrated with historical storms and measured flood levels using the values suggested in Table 2.4S.4-4 (Reference 2.4S.4-10) as initial estimates. The calibrated values are in the range of 0.025 to 0.046 for the river channel and 0.045 to 0.100 for the overbank areas, and they were used in the Halff study to model flood conditions up to the SPF. The extensions in the dam break model adopted the same Manning's *n* values assigned to the boundary limits of original cross-sections of the Halff model.

In a dam break event, there could be considerable amount of turbulence and entrainments of debris for many miles downstream of the breached section. In addition, a dam break flood, potentially with entrained debris, could overflow the river banks into the flood plains as well as inhabited areas, where the roughness could be considerably higher than those under severe flood conditions such as a SPF. To account for these conditions, the Manning's *n* values used by Halff in its HEC-RAS model were adjusted upward conservatively by a factor of 2.0 for 4 miles immediately downstream from the each of the failed dams, i.e., 4 miles downstream from Buchanan Dam and Mansfield Dam, respectively. For the rest of the model river reach, the Manning's *n* values were assumed to be 1.2 times that used in the Halff study (Base Case). A sensitivity case was performed using the same Manning's *n* values as in the Halff study, except for a 4-mile distance downstream from Buchanan Dam as well as from Mansfield Dam where the Manning's *n* values were two times the values used in the Halff study (Sensitivity Case). Increasing the Manning's *n* values increases the

simulated water levels because of increased roughness and therefore is a conservative approach in estimating the maximum flooding water levels at the plant site.

2.4S.4.2.1.5 Predicted Water Levels at STP 3 & 4 from Upstream Dam Failure Model

The HEC-RAS dam breach and unsteady flow routing model (Base Case) predicted that the peak water level at the STP site, without considering the wind wave effects, due to the domino-type failure of the upstream dams would be at El. 28.6 ft MSL or 28.4 ft (NAVD 88). The discharge at the time of the peak water level would be 1.87 x 106 cfs. For the Base Case, the flood wave would take about 65 hours to reach STP 3 & 4 after Mansfield Dam fails. This flood wave travel time would be about 58 hours for the Sensitivity Case. The predicted dam break flood and stage hydrographs for the two cases are presented in Figures 2.4S.4-9 and 2.4S.4-10. The simulated maximum dam break water surface profile from Buchanan Dam to the downstream boundary for the Base Case and Sensitivity Case are depicted in Figures 2.4S.4-11 and 2.4S.4-12, respectively.

2.4S.4.2.2 MCR Embankment Breach Analysis

FLDWAV, a computer program developed by the National Weather Service (Reference 2.4S.4-12), was used to generate the outflow flood hydrograph from the MCR embankment breach, based on breach parameters discussed in Subsection 2.4S.4.2.2.2.2. This flood hydrograph was used as input to the two-dimensional flow model downstream of the breach.

RMA2 is a two-dimensional (2-D), depth-averaged finite-element hydrodynamic numerical model developed by the United States Army Corps of Engineers (USACE) (Reference 2.4S.4-12a). RMA2 was used to determine the flood elevations and velocities at the safety-related facilities of STP Units 3 and 4. The computer program can simulate dynamic water surface elevations and horizontal velocity components for subcritical, free-surface flow in a 2-dimensional flow field. The governing equations of RMA2 are the depth-integrated equations of fluid mass and momentum conservation in two horizontal directions. The governing equations are solved by finite-element method using the Galerkin Method of weighted residuals, and the integration in space is performed by Gaussian integration. Derivatives in time are replaced by a nonlinear finite difference approximation. The solution is fully implicit and the set of simultaneous equations is solved by the Newton-Raphson nonlinear iteration scheme. The computer code executes the solution by means of a front-type solver, which assembles a portion of the matrix and solves it before assembling the next portion of the matrix. The Surface Water Modeling System (SMS) (Reference 2.4S.4-12c) was used as the pre-and post-processor for the RMA2 model.

A 2-D model grid was developed based on topographic information and assigned parameters, such as Manning's roughness coefficient. Breach characteristics and a breach outflow hydrograph were incorporated into the 2-D grid, based on the breach analysis and FLDWAV results. A sensitivity analysis was conducted to evaluate the RMA2 results.

The following paragraphs discuss the failure scenarios considered for the initiation of the postulated MCR breach. An overtopping failure of the MCR embankment is not considered because the freeboard above the normal maximum operating level is greater than 15 feet.

The MCR embankment contains an internal drainage system that provides control of through-reservoir seepage and underseepage potential within the embankment. This prevents the phreatic surface (where the hydraulic pressure head is zero) from increasing within the embankment to such a level as to lead to a potential catastrophic exiting of water at the downstream face of the embankment. Since the upstream (reservoir side) of the embankment has a soil-cement facing, seepage potential through the embankment is greatly reduced. However, the failure scenario adopted for this study conservatively assumes that the internal drainage system within the embankment substantially fails to provide its intended seepage relief function. This failure could occur through:

– Disruption of the horizontal drainage blanket through either a seismic event or activity of a growth fault that causes a break in this drain system.

– Blockage of relief wells by debris, rodents, siltation from embankment toedrainage backwater, or other means.

Disruption of the horizontal blanket drains could occur through shifting of the horizontal material layer during a seismic event or through activity of a growth fault. According to Subsection 2.5S.3.8.1, the potential for deformation due to seismic activity at the STP site is negligible, and there are no capable tectonic faults within the site vicinity. The potential for non-tectonic deformation and growth faults at the STP site are discussed in Subsections 2.5S.3.2.2 and 2.5S3.8.2. It was concluded that the potential for permanent ground deformation from activity on the growth fault structure at the site is negligible. Additionally, the potential for non-tectonic deformation at the site and the potential for non-tectonic deformation from movement on growth faults are considered negligible. Therefore, it is very unlikely that a failure of the drainage blanket would occur due to a postulated seismic event or activity due to growth faults.

The blockage of relief wells could conceivably occur if the existing surface drainage system at the toe of the embankment drains slowly or becomes plugged, creating a backwater effect. This backwater situation would allow silt within the standing water to settle, thus filling the drainage outlets. The internal seepage would then build-up within the embankment. This pressure build-up would eventually exit at the downstream toe of embankment. The saturation of the embankment could induce sloughing of the downstream toe section, providing a larger release area and a shorter flow path of seepage. Any free exiting of the seepage flow could allow movement of embankment material with subsequent generation of a piping failure.

The potential for an embankment failure due to piping caused by an uncontrolled water level build-up within the MCR embankment is considered very improbable for the following reasons: the engineered design of the MCR embankment; established operation and maintenance requirements that include embankment inspections and

piezometer monitoring; the low probability of outlet drain plugging due to rodent activity; and the low probability of sediment deposition plugging the outlet drains. Therefore, the postulation of MCR embankment failure by piping is very conservative.

2.4S.4.2.2.1 Assumptions in the MCR Embankment Breach Analysis

The following assumptions were used for the MCR embankment breach analysis:

(1)   For modeling the flood elevation on the site, it was assumed that the large concrete structures such as STP Units 1 and 2 as well as Units 3 and 4, and several other tall and durable structures would remain in place during the flood. Other structures, such as metal skin buildings and warehouses, were assumed to be removed by the high velocity flood flow but have steel framing and associated remaining debris that would result in higher friction to flow. This higher friction to flow was incorporated by using a higher Manning's *n* for those elements.

(2)   The bottom elevation of the MCR ranges approximately between elevations 16.0 ft and 28.0 ft. It was assumed that the average bottom elevation of the MCR is 20 ft (6.1 m), which is a representative low bed level in MCR.

(3)   Breach side slopes were assumed to be 1 vertical to 1 horizontal for FLDWAV modeling.

(4)   During the breach simulation it was assumed that there was no rainfall and therefore, there was no inflow to the MCR.

(5)   It was assumed that the lateral expansion of the breach would occur symmetrically about its centerline.

2.4S.4.2.2.2 FLDWAV Flow Model Simulation

FLDWAV is a parametric, numerical model used to generate the breach outflow hydrograph based on user-input breach parameters. The breach parameters are estimated using empirical equations developed from case studies of historical dam failures.

2.4S.4.2.2.2.1 Initial (Starting) Water Level in the MCR

The starting water level in the MCR considered for the breach analysis was 50.9 feet. This level corresponds to the response of the MCR to one-half PMP on the normal maximum operating level plus the effect of wind set-up produced by the 2-year wind speed (50 mph) from the south (Reference 2.4S.4-7).

2.4S.4.2.2.2.2 Selection of the MCR Embankment Breach Parameters

Reference 2.4S.4-12d by the Dam Safety Office of the U.S. Bureau of Reclamation describes several dam failure case studies that support empirical breach parameter relationships, and is considered the most complete and knowledgeable source for estimation of dam breach parameters. The breach parameters for the MCR

embankment breach analysis were established based on discussions within this reference.

The portion of the northern embankment in line with and due south of Units 3 and 4 is the closest to the units, and therefore is considered the most critical location for a breach of the MCR embankment, with respect to flooding at STP 3 & 4. The top elevation of the embankment in this area is approximately El. 65.75 ft. A service road runs along the toe of the exterior slope of the MCR northern embankment. Due to an anticipated large scour hole that would occur at the breach location, it was assumed that the road would be eroded. The terrain immediately downstream of the road is considered to be the control for the breach bottom elevation. Therefore the breach bottom elevation was taken to be at El. 29 ft. Breach side slopes were taken to be 1 horizontal to 1 vertical, a ratio consistent with observations for earth-filled structures described in Reference 2.4S.4-12d.

Reference 2.4S.4-12d by the Dam Safety Office of the U.S. Bureau of Reclamation describes several dam failure case studies that support empirical breach parameter relationships. This reference describes several methods for estimating breach parameters. These methods include:

– Physically Based Methods: predicting the development of a breach and resulting outflow through use of an erosion model based on principles of hydraulics, sediment transport and soil mechanics.

– Parametric Models: using case studies of known dam failures to estimate time to failure and final breach geometry, then using these estimates within a computer model using principles of hydraulics.

– Predictor Equations: estimating peak discharge from empirical equations based on case studies of known dam failures.

– Comparative Analysis: using the breach shape and peak outflow of a dam that was of similar size and construction that had failed.

Physically based methods incorporate sediment transport and soil mechanics. In general, most of the available numerical dam breach models rely on bed-load type erosion formulas that utilize assumptions of gradually varied flow and relatively large flow depth in comparison to the size of roughness elements. These formulations are not consistent with the mechanics of the breaching process as observed in the field and in the laboratory. The other three methods listed above rely on case study data for selection of appropriate equations or parameters. In general, the database of welldocumented dam failure case studies is small and contains few examples of very large storage volumes such as the Main Cooling Reservoir.

Of the various methods, the parametric model method is the most generally utilized method, the method having the greatest research, and the method fully described within Reference 2.4S.4-12d. Table 2 of Reference 2.4S.4-12d describes nine dam failure case studies that lead to empirical breach parameter relationships. The breach parameters consisting of breach bottom width, time to fail, and breach side slopes were

established based on discussions within Reference 2.4S.4-12d, engineering judgment, and the comparison to the Teton Dam failure. Of all the dam failures presented in Reference 2.4S.4-12d, the Teton Dam failure was chosen for comparison because the failure mode was piping and the Teton Dam reservoir had one of the largest storage volumes presented, similar to the MCR. The storage volume in the Teton Dam reservoir was approximately 1.5 times the storage volume in the MCR, and the Teton Dam had a significantly larger breach height of 254 feet versus 21.9 feet in the MCR. Each parameter is estimated independently and conservatively for use in FLDWAV.

The breach bottom width was based on Froehlich (1995b), presented in Reference 2.4S.4-12d. Froehlich's equation, shown in Table 2.4S.4-5, predicts the largest breach width estimate of all methods presented in Reference 2.4S.4-12d. Froehlich's equation provides conservative breach width results in comparison with breach widths from observed dam failures. For example, Froehlich's equation predicts an average breach width of 220 m (722 ft) for the Teton Dam. However, the actual average breach width of Teton Dam at failure was only 151 m (495 ft). Therefore, the breach width determined for the MCR embankment using Froehlich's equation is considered conservative. Froehlich's equation predicts an average breach width of 417 feet. Given the trapezoidal geometry of the breach, the average breach width of 127 m (417 ft) yields a bottom breach width of 116 m (380 ft = 417 - 2(65.75 -29) / 2)), which was used for FLDWAV embankment breach modeling.

Time to fail was based on the equation given by MacDonald and Langridge-Monopolis (1984) presented in Reference 2.4S.4-12d. This equation, shown in Table 2.4S.4-5, predicts a time to fail that came closest to describing a breach expansion rate meeting that of Teton Dam. Breach expansion rate is determined using the predicted breach width and the time to fail. Typical rates of expansion vary from 60 feet lateral per hour to 120 feet lateral per hour. Teton Dam displayed a fairly rapid rate of breach expansion. Based on information presented in Reference 2.4S.4-12d, the time from beginning of rapid growth of breach to significant lateral erosion process stopping at Teton Dam was estimated at 1.25 hours and the final breach width was 496 feet, resulting in an expansion rate of 198 feet per hour. This rapid rate of erosion was due to the higher hydraulic depth to drive the outflow and associated erosion. The MacDonald and Langridge-Monopolis equation predicts a time to fail of 1.7 hours for the MCR. This gives a breach expansion rate for the MCR of approximately 112 feet lateral per hour, which is smaller than the Teton Dam and considered acceptable.

Finally, the breach side slopes were assumed to be 1 vertical to 1 horizontal. This ratio is consistent with all researchers' observations for earth-filled structures, as discussed in Reference 2.4S.4-12d.

Table 2.4S.4-5 presents empirical equations from Reference 2.4S.4-12d and the resulting breach parameters.

2.4S.4.2.2.2.3 MCR Embankment Breach Outflow Hydrograph

The outflow hydrograph from the MCR embankment breach, generated by FLDWAV based on the aforementioned initial conditions and breach parameters is presented in Table 2.4S.4-6. The peak breach outflow predicted by FLDWAV is 130,000 cfs.

The peak discharge predicted by FLDWAV is compared to peak discharge estimates from other methods. Reference 2.4S.4-12d states that the Froehlich equation as shown in Table 2.4S.4-5 is one of the better available methods for prediction of peak breach discharge, because it correlates well with observed dam failure peak flow rates. The peak discharge estimated using Froehlich's equation is 62,600 cfs. The relationship of estimated peak discharges associated with the respective hydraulic head at time of failure from Reference 2.4S.4-12e is given in Figure 2.4S.4-13. From this figure, the peak flow for the MCR embankment breach is only 20,000 cfs, compared to 130,000 cfs as determined by the FLDWAV program. Therefore, the outflow hydrograph with a peak outflow of 130,000 cfs used in the breach analysis is conservative. To further verify the conservatism of the breach parameters and FLDWAV results, an independent analysis of the MCR embankment breach was performed using the BREACH model (Reference 2.4S.4-12e(1)) to predict the breach development and outflow hydrograph. This analysis is presented in Subsection 2.4S.4.2.2.2.4.

2.4S.4.2.2.2.3.1 Sensitivity Analysis of FLDWAV Parameters

A sensitivity analysis was performed on the breach parameters selected for use in the FLDWAV model. The time to fail and the breach bottom width were tested separately to determine the effect of these parameters on the peak discharge predicted using FLDWAV. The results of the sensitivity analysis are shown in Table 2.4S.4-6a.

The data shown in Table 2.4S.4-6a indicates that the breach width has a significant effect on peak discharge. This is reasonable since the large storage to height ratio of this structure would allow little change to the hydraulic head due to volume loss of the breach hydrograph for any of the breach widths analyzed. Therefore, the change in breach width would produce a directly proportional change in breach area, which would in turn produce a directly proportional change in peak discharge.

Timing does not appear to be a significant factor. Lengthening the time to fail reduces the peak discharge; however, this reduction is slight. The results of the sensitivity of these parameters indicate that the peak breach outflow is more sensitive to changes in breach width than to the time to fail, or the breach formation time.

2.4S.4.2.2.2.4 Confirmatory Analysis Using the BREACH Model

To verify the conservatism of the selected breach parameters and the FLDWAV results, an independent, confirmatory analysis of the MCR embankment breach was performed using the BREACH model. BREACH is a physically based mathematical model used to predict the breach development (breach size and time of formation) and the outflow hydrograph from the predicted breach of an earthen dam embankment (Reference 2.4S.4-12e(1)). Input data used by BREACH include embankment

geometry and material properties, reservoir surface area-elevation relationship, and hydraulic characteristics of the channel formed directly downstream of the breach. BREACH couples the conservation of mass and momentum of the reservoir storage and breach outflow with the sediment transport capacity of the unsteady uniform flow along the breached channel. The growth of the breach is dependent on the dam embankment material properties (unit weight, friction angle, cohesive strength and particle size D50, for which 50 percent of the soil particles in the embankment material are smaller). The model simulates the development of the breach through the mechanism of one or more sudden structural collapses that occur when the hydrostatic force exceeds the resisting shear and cohesive forces; enlargement of the breach width by slope stability theory; and initiation of the breach via piping with subsequent progression to a free surface breach flow. For the BREACH model analysis, piping is considered as the breaching mechanism.

2.4S.4.2.2.2.4.1 Assumptions used in the BREACH Model Analysis

The following assumptions were used for the BREACH model analysis of the MCR embankment:

(1)   It is assumed that the lateral expansion of the breach will not be limited geologically or structurally to either the right or left of centerline.

(2)   It is assumed that the piping starts at elevation 34.0 feet, which is the approximate centroid of the initial saturated zone in the failure scenario.

(3)   The downstream control location was assumed to be the ditch along a service road. Due to an anticipated large scour hole that would occur downstream of the breach location, the slightly perched road was assumed to be removed by erosion and the natural terrain immediately downstream of the road considered to be the control for the breach bottom elevation of 29 feet. A Manning's roughness coefficient of 0.06 was conservatively selected for the downstream channel routing reach. This reach has service roads, ditches, and small buildings that provide a roughness condition that would support the selected roughness coefficient. The downstream bottom slope was assumed to be 8 feet per mile.

(4)   The cross section of the embankment has a berm on the downstream slope at approximately elevation 35 feet. This berm extends outward approximately 45 feet with a 6H:1V down slope. It was assumed that a potential breach mechanism would be an embankment slope failure that would, effectively, remove the berm altogether. Therefore, no effort was made in describing this berm cross section within the BREACH model. This is a conservative assumption.

(5)   The soil cement protective layer on the upstream slope of the embankment was not considered in the BREACH model. The assumed piping failure would generate a head-cut progressing from downstream to upstream. The head-cutting action would remove the material from behind the soil cement protection layer, undermining the slope protection. Since soil cement has little

tensile strength, the soil cement would not be able to maintain its integrity when unsupported. However, it would be reasonable to expect that the soil cement would not crumble immediately but would require some time after a piping failure has progressed. In addition, the effect of the soil cement liner is to decrease the breach erosion rate and hence increase the time to peak, resulting in a decreased peak breach outflow rate. Therefore, it is conservative to exclude consideration of the soil cement liner.

2.4S.4.2.2.2.4.2 Sensitivity Analysis of BREACH Model Inputs

A sensitivity analysis was performed on selected embankment material parameters. The unit weight, internal friction angle and cohesive strength are based on field measurements or laboratory testing, and therefore sensitivity analyses were not performed for these three parameters.

It was found that varying both the critical shear stress coefficient and the critical stress coefficient (C_a and C_b) within their respective ranges recommended in Reference 2.4S.4- 12e(1) had no effect on the predicted peak breach discharge. Also, varying the plasticity index (PI) from 0 to 40 had no effect on the predicted peak discharge. Decreasing the value of D50 to that of a fine clay material (0.0001 mm) increased the peak discharge by less than a percent. Therefore, the peak breach discharge is not considered sensitive to these four parameters.

Changing the ratio of D_{90} (the soil particle size for which 90 percent of the embankment material is smaller) to D_{30} (the soil particle size for which 30 percent of the embankment material is smaller) by a factor of two either way changed the peak discharge by about 3 percent and hence was considered non-sensitive. Using a D_{90} to D_{30} ratio of 16 produced a higher discharge, but this ratio would indicate a well-graded material, which is not the case for the embankment material. The porosity ratio also was found to have a fairly insignificant effect on the breach outflow results. The 0.35 porosity ratio used is considered to be an upper end value. A compacted soil porosity value of 0.20 would be reasonable to assume for the embankment. Using a porosity ratio of 0.20 reduced the peak discharge by about three percent. Therefore, the higher porosity value of 0.35 was considered to be conservative.

Of all the parameters, the Manning's n-value has the greatest effect on the predicted peak discharge. The Manning's n-value within the BREACH model is computed using the Strickler relation of roughness to the average grain size (D_{50}). The formula is defined as follows (Reference 2.4S.4-12e(1)):

$$n = 0.013 * (D_{50})^{0.67}$$

This formula produced an n-value of 0.001 for the MCR embankment. This value is unrealistically low. While using the BREACH model for Teton Dam breach analysis, Fread (Reference 2.4S.4-12e(1)) commented that the Strickler equation was judged not to be applicable for the fine breach material and used a relatively higher n-value of 0.013 for the analysis. For the present analysis a range of n-values were tested.

N-values similar to those for a natural channel with clay material on all sides of the flow path were estimated based on engineering judgment and methods developed by others, such as Ven te Chow (Reference 2.4S.4-12e(2)). Using Table 5-5 within Reference 2.4S.4-12e(2), the n-value based on an earthen channel would be 0.02. Applying an additional 0.005 for irregularity of the flow channel, a combined total n-value of 0.025 was considered. The degree of irregularity and variation in cross section may be such that the overall n-value could be doubled, for an upper end value of 0.05. Therefore, an n-value within the range from approximately 0.025 to 0.05 was considered reasonable.

The BREACH algorithms are such that the lowest n-value considered, 0.025, produced a lower peak discharge than the highest n-value considered, 0.05. Therefore, consideration was given to a higher n-value of 0.08 that was still considered within the range of feasibility. Table 2.4S.4-6b presents the predicted peak discharge, breach width at time of peak discharge, time to peak discharge and reservoir level at time of peak discharge for each of the three n-values modeled. Figure 2.4S.4-13(a) presents the breach width development over time for all three n-values tested. The results of the sensitivity analysis indicate that higher roughness coefficients produce higher peak discharge values, which is counterintuitive. One explanation for this may be attributed to the model predicting a sudden collapse of the pipe section of the dam sooner with the lower n-values, thus lowering the peak discharge at a critical time. It is noted that the peak discharge and breach opening rate is based on several modeling algorithms that are balancing discharge forces, sediment transport rates and structural features with predicted storage depth and tailwater depth. An n-value of 0.05 is used in the FLDWAV analysis.

2.4S.4.2.2.2.4.3 BREACH Model Results and Comparison with FLDWAV

The BREACH model results showing breach width development with respect to time of breach formation are presented in Figure 2.4S.4-13(b). The breach width increases initially at a fairly constant rate for the first five hours, after which the rate of breach expansion decreases. The peak discharge of approximately 83,200 occurs when the breach bottom width is 361 feet. The reservoir water level continues to drop as water flows out of the reservoir through the breach and the downstream channel erodes as it carries the large outflow from the breach. It is noted that the rate of erosion would decrease substantially after the first five hours of the breach process. However, considering the large volume of water remaining in the MCR, the breach continues to expand with diminishing outflow and a decreasing breach width erosion rate. The final breach width reached after 30 hours is 448 feet.

Table 2.4S.4-6c and Figure 2.4S.4-13(c) provide a comparison of the results from BREACH and FLDWAV. The breach width and time to peak used as input to the FLDWAV program were conservatively estimated based on case studies of historical dam failures presented in Reference 2.4S.4-12d. FLDWAV assumed a linear increase of the breach bottom width from 0 to a maximum width of 380 feet in 1.7 hours, which is the time the peak outflow occurs. The BREACH model produced the peak discharge 6.25 hours after the start of the breach development and allowed the breach width to continue to expand after the peak discharge. The BREACH model estimates a lower

peak discharge as compared to the peak discharge predicted using the FLDWAV model. Even using an unrealistically high n-value of 0.08, the BREACH peak flow results are lower than the peak flow obtained with the FLDWAV model.

The BREACH model provides an independent assessment of the postulated breach of the MCR embankment at the STP 3 and 4 site. The BREACH model estimates a longer time to peak and a narrower breach width at the time of peak compared to the parameters selected for use in the FLDWAV model. BREACH also predicted a lower peak discharge than the peak discharge predicted using the FLDWAV model. Therefore, the parameters selected for FLDWAV and predicted breach hydrograph are considered conservative and acceptable.

2.4S.4.2.2.3 RMA2 Two-Dimensional Model Simulation

After developing the maximum credible breach scenario, resulting hydrograph and resulting embankment erosion rates, the next step is to route the breach hydrograph to the safetyrelated facilities. Because of the complex topography of the site, a 2-dimensional (2D) simulation was considered appropriate. RMA2 has been used widely to conduct dynamic simulations of water level and velocity distribution in rivers, reservoirs, and estuaries, and is considered an acceptable tool to model the flood flow from the MCR embankment breach.

2.4S.4.2.2.3.1 Bathymetry Elevations and Two-Dimensional Grid Development

The topography of the STP site was used to determine model bathymetry for routing the flood flow resulting from the MCR embankment breach. The 2-D grid was developed using: (1) STP Site Topography; (2) STP Units 3 and 4 Site Grading Plan; and (3) STP Units 3 and 4 Plot Plan. The grading plan around Units 3 and 4 power block site is shown in Figure 2.4S.4-14. The grade elevation at the center of the power block is EL. 36.6 ft and slopes to El. 32 ft at the four corners. Facilities included in the model grid are the Reactor, Turbine, Control, Radwaste, Service and Hot Machine Shop buildings for Units 1 through 4. The Ultimate Heat Sinks for Units 3 and 4 and Essential Cooling Pond (ECP) for Units 1 and 2 were also included in the model grid.

The datums of the 2-D grid are in NAD 27 State Plane Texas South Central for the horizontal datum and NGVD 29 for the vertical datum. The northern embankment of the MCR was selected as the southern boundary of the 2-D grid, and road FM 521 was chosen as the northern boundary of the grid. The western and eastern boundaries of the grid were selected to be sufficiently far from Units 3 and 4 so the target area is not impacted by the model boundaries (Figure 2.4S.4-15).

To assist the 2-D model stability associated with the wetting and drying of model elements and to further ensure that the target area is not impacted by model boundaries, a hypothetical sump was modeled along the east, north, and west boundaries of the developed 2-D grid outside of FM-521. The use of the sump to help with model stability is a common practice in the 2-D modeling field. Reference 2.4S.4-12e3 and Reference 2.4S.4-12e4 describe the use of sumps in physical models to control (and vary) the boundary conditions for calibration and the concept of "hybrid modeling" where results from a physical model of a complex region are used as input

or boundary conditions for a comprehensive numerical model. References 2.4S.4-12e5 through 2.4S.4-12e8 show precedents for the use of artificial sumps in RMA2 applications. The sensitivity analysis described below indicates that the hypothetical sump has no impact on model results in and around Units 3 and 4. As a result, the developed 2-D grid (excluding the artificial sump area) covers an area of 1,477 acres: 5,873 ft in the north-south direction, and 12,455 ft in the east-west direction. Figures 2.4S.4-16 and 2.4S.4-17 show the 2-D grid with elevations for the east breach and west breach, respectively. The sump is the deeper area on the outside of the model grid. The 2-D grid includes 2,348 nodes and 1,088 elements. The size and location of these elements were selected to best represent physical features, particularly around Units 3 and 4. The areas of the 2-D elements range from about 2,500 square feet near the reactor buildings to about 144,000 square feet away from the units.

2.4S.4.2.2.3.2 Manning's Roughness Coefficients

The Manning's roughness coefficient (*n* value) for each model element was assigned based on typical values published by the United States Geological Survey (USGS) (References 2.4S.4-12f and 2.4S.4-12g) and the HEC-RAS manual (Reference 2.4S.4-12h). Each major building was evaluated on whether it would remain in place following the flood caused by a MCR embankment breach. Those buildings that were assumed to remain in place were considered "hard buildings." Any hard buildings higher than elevation 62 feet were considered to be a total blockage to the flow, and therefore were shown as blank areas in the 2-D grid. Those buildings assumed to fail were considered "soft buildings." Soft buildings were assumed to be destroyed with foundation slab remaining in the grid. These buildings were considered "high drag" areas with a higher roughness value to represent the effects of remaining frame and debris. Any buildings not included in the 2-D grid were represented by a higher Manning's n value. Due to the resolution of the grid, the Vehicle Barrier System around the power blocks was not built into the grid, but instead was represented by higher Manning's *n* value. Manning's n values assigned to each material type are listed in Table 2.4S.4-7. Figure 2.4S.4-18 shows the material types assigned to various elements in the 2-D grid. These Manning's *n* values were conservatively determined for each type of surface.

2.4S.4.2.2.3.3 Boundary Conditions

The downstream boundaries of the model were positioned far enough downstream so that the maximum flood level at the STP Units 3 and 4 safety-related buildings due to a MCR embankment breach would occur before the flood front reaches the two boundaries. A constant water surface elevation was defined for the downstream boundary condition. A sensitivity analysis was performed on the downstream boundary condition, as discussed in Subsection 2.4S.4.2.2.4.1.

2.4S.4.2.2.4 Results of MCR Embankment Breach Analysis

2.4S.4.2.2.4.1 Water Levels and Velocities

Critical STP 3 and 4 site locations for RMA2 model results are shown on Figure 2.4S.4-19. To determine the maximum effect on each of the Units 3 and 4, separate east and west breach locations were simulated. The variation in water surface elevation at these locations from 1.2 hours to 2.5 hours of the model simulation are presented in Figures 2.4S.4-20 and 2.4S.4-21 for the east breach and west breach, respectively. This selected period includes the peak water level and peak velocity near the plant buildings. The peak water level of 38.8 feet occurred at the Unit 4 Ultimate Heat Sink structure for the west breach scenario. Peak water surface elevations for the east breach and west breach are shown on the plan grid in Figures 2.4S.4-21(a) and 2.4S.4-21(b), respectively. Peak velocities associated with the east breach and west breach are shown in Figures 2.4S.4-21(c) and 2.4S.4-21(d), respectively. The maximum velocity of the flood flow was found to be 4.72 feet per second and occurred between Units 3 and 4 (point 8 on Figure 2.4S.4-19). The variation in velocity at locations 1 through 8 for the period containing peak velocities for the east and west breach scenarios is shown in Figures 2.4S.4-21(e) and 2.4S.4-21(f), respectively.

As discussed above, the flood simulation provides peak water depth and peak velocity values at critical STP 3 and 4 site locations. Peak flood discharges per unit width near the power block buildings may be estimated using these values. Table 2.4S.4-7a provides examples of peak discharge per unit width estimated for locations near the Unit 4 UHS, the power block on the south side of Unit 4, and at a location between Units 3 and 4. These estimates are based on the west breach simulation results for peak water surface elevation and peak velocity, as shown in Figures 2.4S.4-21 and 2.4S.4-21(f), respectively. The water depths are obtained by subtracting the nominal site grade elevation in the power block of 34 feet from the peak flood water surface elevations.

A sensitivity analysis was conducted to determine the effect of boundary condition on the resulting water levels. The analysis indicated that changing the water surface elevation at the downstream boundary from 32.5 feet to 34 feet does not affect the peak flood levels for the site.

2.4S.4.2.2.4.2 Effects of Sedimentation and Erosion

The MCR embankment breach analysis also considered the material eroded during the breach. The embankment material eroded is comprised mostly of clay, with a small percentage of sand from the internal drainage system and soil cement from the interior embankment slope lining. The erosion process will also produce a scour hole downstream of the breach that extends below the breach bottom elevation. The dimensions of this scour hole, based on lab results from Reference 2.4S.4-12i, are estimated to be 20 feet deep, 203 feet long and 380 feet wide. The scour hole contributes 1,543,000 cubic feet of clay to the flood flow. The material eroded from the MCR embankment contributes an additional 1,697,314 cubic feet of clay; 75,644 cubic feet of sand; and 117,562 cubic feet of soil cement. The total volume of sediment eroded under the breach scenario is 3,433,517 cubic feet.The flood flow from the MCR

embankment breach would not cause erosion at the STP 3 and 4 plant site area because surfacing in this area is mostly concrete or asphalt pavement or compacted stone surfacing. The maximum velocity of 4.72 ft/s would not cause severe erosion of these surfaces, and any minor erosion around corners of the buildings would not impact the safety-related facilities of Units 3 and 4. Therefore, the power block surfacing would remain intact following the MCR embankment breach flood.

It is anticipated that sedimentation will not have a significant effect on the site and the maximum water level resulting from the MCR breach flood. The majority of the clay and sand loads would be suspended in the flood flow and washed downstream, north of FM 521 and beyond the STP site. The soil cement lining on the interior wall of the embankment would likely enter the water as chunks or blocks as the embankment collapses, and these large concrete blocks would be carried only a short distance from the breach before settling to the bottom. The sediment loading would cease when the breach opening expansion ends; however, low-sediment flows would continue for a number of hours afterwards until the water in MCR is totally emptied. This continued flow period would prevent any remaining clay or sand particles from settling and would wash away any small depositions in the study area.

RMA2 does not have sediment transport modeling capabilities, thus a bounding analysis was performed to determine a conservative sediment accumulation depth within the Units 3 and 4 power block area. This analysis is based on conservatively assuming twice the calculated total sediment volume from the MCR breach and scour hole and applying it on a fan area (potential sediment deposition area) extending from the breach to the peripheral road to estimate the maximum sediment depth near the plant area. Though the sediment material is primarily clay, most of which would remain in suspension, it is assumed for this bounding analysis that all the material settles uniformly within the fan area.

The analysis includes both the east and west breach scenarios. For each of the scenarios, a sediment fan area is considered that extends from the MCR breach to FM 521. The fan areas, shown in Figure 2.4S.4-21(f1), were selected by reviewing the RMA2 flow fields so that the fan areas follow the main path of the simulated breach flows. The total area of selected 2-D elements within a fan area is reported automatically by SMS. The building areas are excluded from the area calculations. The total volume of sediment material considered for this analysis is 6,867,040 cubic feet. The areas of the fans for the east and west breach scenarios are 19,646,580 square feet and 17,948,623 square feet respectively. The estimated sediment depths within the fan areas are 0.35 feet and 0.38 feet for the east and west breach scenarios, respectively.

The bounding analysis shows that the sediment depths near the power block would be in the range of 0.35 to 0.40 feet. Even with the sediment depth of 0.4 feet, and further assuming that the flood water elevation were raised by the same amount, the maximum water level due to MCR breach flood would be 39.2 feet instead of 38.8 feet. The design basis flood level of 40 feet for the STP Units 3 and 4 will not be affected due to sedimentation.

2.4S.4.2.2.4.3 Hydrodynamic Forces

The maximum water levels and velocities obtained near Units 3 and 4 were used to assess the hydrodynamic loadings on the plant buildings. Figures 2.4S.4-21(e) and 2.4S.4-21(f) show the time-dependent plots of the velocities during the east and west breach scenarios, respectively. The peak velocities observed in between Units 3 and 4 were 4.72 and 4.68 feet per second for the east and west breach scenarios, respectively. The sediment loads associated with the flow from the MCR embankment breach were developed to determine sediment concentrations and the sediment-laden water density. The time-dependent, well-mixed sediment concentrations were obtained assuming that no sediment gets transported outside of the study domain. The sediment concentration corresponding to the peak velocity occurring at T=1.7 hours was 22.33 kg/m3. Therefore, a sediment concentration of 23 kg/m3 was used to determine the sediment-laden water density. With a sediment concentration of 23 kg/m^3, a water density of 1023 kg/m^3 or 63.85 lb/ft^3 was used for load calculations. The maximum hydrostatic force on any plant building would be due to the depth of floodwater at the maximum water level.   Hydrodynamic loads were calculated using the drag force formula with a drag coefficient conservatively set to 2.0, as presented below:

$$\text{Force (lb/ft}^2) = 2.0 \times \text{Density (lb/ft}^3) \times \text{Velocity}^2 \text{ (ft}^2/\text{sec}^2) / 2g$$

The maximum drag force due to the maximum velocity of flow near the plant buildings is estimated as 44 pounds per square foot of the projected submerged area of the buildings.

The hydrodynamic loads due to wind-generated waves have also been calculated. A two year fastest mile wind speed of 50 mph, based on Reference 2.4S.4-7, is conservatively applied coincident with the Main Cooling Reservoir (MCR) breach flood level. The methodology given in the Coastal Engineering Manual (CEM), Reference 2.4S.4-13, is used to estimate the wave height and wave forces on the vertical walls of the power block buildings.

Based on the site layout and considering the sheltering effect of other buildings or structures on the site, the controlling fetch length will be due to the westerly winds. Therefore, the longest fetch on the west facing Unit 4 safety-related structures is determined. For this governing condition, the wave height is calculated for the above wind speed, fetch and the depth of water along the fetch. Based on this, a significant non-breaking wave with a wave height (H_s) of 1.25 feet and a period (T) of 1.7 seconds would be generated. Considering a 1% wave height ($H_1 = 1.67\ H_s$) of 2.1 feet, per Reference 2.4S.4-7, the wave force due to the wind generated waves is calculated and conservatively applied to all the safety-related structures including those for Unit 3.

The resultant hydrodynamic wave force is calculated to be 603 pounds (0.6 kips) per foot length of the vertical wall corresponding to the maximum breach flood level of 38.8 feet. The wave force diagram is shown in Figure 3.4-1.

Due to the waves generated by the postulated wind the water level near the safety-related structures will fluctuate above and below the still water level caused by the

MCR dike breach flood. As stated above, the water levels near the Unit 4 safety-related structures are affected more than the water levels near the Unit 3 structures due to the controlling westerly winds. Therefore, the rise in water level due to wind wave effect near Unit 4 safety-related structures is considered as the upper bound water level fluctuation for the Unit 3 structures also.

Following are the maximum water levels near Unit 4 safety-related structures due to MCR dike breach flood and the fluctuation of the water level due to the wind waves. The MCR dike breach flood levels are described in Section 2.4S.4.

– Maximum water level due to MCR breach flood near the Unit-4 Ultimate Heat Sink (UHS) = 38.8 feet

– Maximum water level due to MCR breach flood near the Unit-4 power block structures = 38.2 feet.

– Maximum periodic rise in water level due to wind wave action = 3.1 feet (see Figure 3.4-1)

Including the fluctuation in water level due to wind wave effect;

– The maximum water level near the Unit-4 UHS = 38.8 + 3.1 = 41.9 feet.

– The maximum water level near the Unit-4 power block structures = 38.2 + 3.1 = 41.3 feet.

The UHS and Reactor Service Water (RSW) Pump Houses are designed to be watertight below 50 feet MSL. All the power block safety-related structures are watertight below elevation 41.0 feet MSL due to one foot threshold provided above the design basis flood level of 40 feet MSL. Any periodic splash flooding above the 41-foot elevation up to the wave run-up elevation of 41.3 feet MSL will be minor and would be taken care of with normal housekeeping and will not affect the safety-related function of the structures.

2.4S.4.2.2.4.4 Spatial Extent of Flooding Due To MCR Embankment Breach

For both the east and west MCR embankment breach scenarios flood water from the breach opening will flow through the area encompassing Units 1 and 2 and Units 3 and 4, and will spread into the area bounded by FM 521. The model simulations end at the boundary cells immediately outside of FM 521. This road has a top of road elevation of approximately 28 feet to 30 feet, as seen from the USGS topographic map of the area (Figure 2.4S.4-21(i)). North of FM 521 and west of the west MCR embankment there are levees with approximate top elevations of 29 feet to 30 feet. South of the MCR along its south embankment is an east - west canal with levees on both sides. The area around the STP plant has an approximate grade elevation varying from 25 feet to 30 feet.

The area around the STP plant slopes east towards the Colorado River. Therefore, most of the flood water from the breach would flow to the Colorado River. A portion of

the breach flow will also reach the Little Robins Slough to the west, which flows south along the west MCR embankment. From there, the water will either flow east to the Colorado River or will flow under the east-west canal through existing siphons and may flow through several swampy areas to the intracoastal waterway.

A small portion of the breach flood flow may reach the Tres Palacios River to the west of the STP site.

2.4S.4.2.2.4.5 Duration of Inundation at Safety-Related SSCs

The duration of inundation at the power block is considered to be the duration during which the flood elevations are greater than the grade elevation of 34 feet. Since the primary purpose of the breach flood modeling was to determine the maximum flood elevation at safety-related facilities, the simulation was terminated after the maximum flood elevation was reached, well before all the water had drained from the site. As a result, a full RMA2 simulation for the duration of the flood water above elevation 34 feet was not performed. However, a reasonable estimate of this duration of inundation can be obtained by relating the resulting flood elevations generated from the RMA2 run to the corresponding flow rates from the breach outflow hydrograph, occurring at the same time. The flood elevations and outflows are plotted on the same graph with time as the common base, as shown in Figure 2.4S.4-21(j). Extrapolated flood elevations were estimated by fitting a non-linear polynomial regression curve. The time elapsed between the two points corresponding to a flood elevation of 34 feet at the power block is estimated at 20.5 hours. Therefore, the estimated duration of inundation (above 34 feet) at safety-related SSCs is 20.5 hours.

2.4S.4.3 Water Level at the STP 3 & 4 Site

Analyses of the dam failures on the Lower Colorado River and the failure of the MCR northern embankment showed that the critical flood level of the safety related structures is controlled by the MCR embankment failure. The design basis flood level for the safety related facilities of STP 3 & 4 is conservatively established as 40.0 ft MSL as discussed below.

2.4S.4.3.1 Water Level at the STP 3 & 4 Site from the Failures of Upstream Dams

In accordance with the guidelines in ANSI/ANS-2.8, Reference 2.4S.4-7, the maximum dam breach flood level at the plant site needs to consider the wind setup and wave runup effect from the coincidental occurrence of a 2-year design wind event. The 2-year fastest mile wind speed at the site is 50 mph based on Reference 2.4S.4-7. The methodology given by the Coastal Engineering Manual (CEM), Reference 2.4S.4-13, was adopted to estimate the wave height and wave run-up at STP 3 & 4 power block. The procedures outlined in CEM use the wind speed, wind duration, water depth, and over-water fetch distance, and the run-up surface characteristics as input. As discussed in UFSAR for STP 1 & 2 (Reference 2.4S.4-5), accurate estimates of the fetch length for this flooding scenario could not be made. Based on the topographic variations and any man-made features that would limit wind effects, however, two critical fetches were identified as shown in Figure 2.4S.4-22; one in an easterly direction towards a low lying ridge and the other along the Colorado River in a northeasterly direction. The fetch in the easterly direction was estimated to be about

15.5 miles with a maximum water depth varying from 1 to 23 ft at the peak of the dam break flood. The fetch along the northeasterly direction was estimated to be about 17.6 miles, with a maximum water depth varying from 1 to 9 ft at the flood peak.

The maximum wind set-up for the critical fetch lines was estimated using a method suggested in Reference 2.4S.4-14, and was found to be about 3.9 ft. Adding to the maximum water level of El. 28.6 ft MSL, estimated by the HEC-RAS dam break model for the STP site, the water level from the dam failure flooding scenario would therefore be at El. 32.5 ft MSL. With the surrounding site grade around the power block and UHS at a nominal elevation of 28.0 ft MSL, the water depth approaching at the STP power block and UHS would be about 4.5 ft. At this shallow depth, a breaking wave condition would prevail and a breaking wave index of 0.78 was used in estimating the break wave height. The breaking wave setup is typically small and is assumed to have a negligible impact on the flood level.

All the safety-related facilities including the UHS are located in the power block island. The power block island will have a grade elevation of approximately 34.0 ft near the plant buildings and will slope towards the periphery to an elevation of 32.0 ft at the edges. The outward slope of the island will be at 10H:1V from elevation 32.0 ft to an existing grade elevation of 28.0 ft.

The maximum wave run-up was estimated using the breaking wave height of 3.5 ft and a maximum wave period equal to 1.2 times of the significant wave period which was estimated to be 3.7 seconds. Conservatively assuming that the run-up surface is smooth, impermeable and using a slope of 10H:1V for the power block island, the wave run-up was estimated to be 1.9 ft.

The maximum flood level at STP 3 & 4 power block as a result of the probable worst case dam failure scenario coincidental with a 2-year design wind of 50 mph was estimated to be at El. 34.4 ft MSL. Table 2.4S.4-8 presents the water levels due to dam break, wind set-up and wave run-up at STP 3 & 4 for the critical fetch.

Because the STP is about 300 miles from Mansfield Dam, any dynamic effects of the dam break waves would have been attenuated along this distance. Therefore, the dynamic effects of the dam break flood waves are not the controlling design criterion of the safety related facilities.

2.4S.4.3.2 Water Level at the STP 3 & 4 Site from Breaching of MCR Embankment

The maximum water level at STP 3 & 4 is governed by the postulated breaching of the MCR's northern embankment. The design basis flood level at the power block and UHS of STP 3 & 4 based on the breaching of the MCR's northern embankment is at El. 40.0 ft MSL. Because the design basis flood level is higher than both the nominal plant grade of 34.0 ft MSL and the entrance level slab elevation of 35.0 ft MSL for the STP 3 & 4 safety related facilities, all safety related facilities are designed to be water tight at or below elevation 40.0 ft MSL. All ventilation openings of safety buildings are located at 40.0 ft MSL or above. Flood protection design is discussed in Subsection 2.4S.10 and Section 3.4.

2.4S.4.3.3 Sedimentation and Erosion

During an upstream dam failure event, because the plant site is located in the floodplains of the Colorado River, the flow velocities are expected to be relatively small compared to that in the main channel. In addition, the flow depths on the floodplain are shallower to effect any significant erosion that would impact the safety of the plant. Although some sedimentation may occur near the plant site, the safety related structures and functions would not be affected by siltation because they are located at higher grades than the surrounding area.

The erosion and sedimentation during a MCR embankment breach event is discussed in Subsections 2.4S.4.2.2.4.2 and 2.4S.10.

2.4S.4.4 References

2.4S.4-1   "Texas Administrative Code – Title 30, Part 1, Chapter 299," Office of the Secretary of State of Texas, provisions adopted to be effective May 13, 1986 (11 TexReg 1978).

2.4S.4-2   "Phase II – Dam Safety Evaluation Project, Task Order B – Reconnaissance investigation, Interim Report," Volume I, Freese and Nichols, Inc., August 1992.

2.4S.4-3   "Celebration marks completion of 10-year LCRA dam project to improve public safety," Press Release by LCRA dated January 12, 2005; available at http:/www.lcra.org/newsstory/2005/dam_upgrade_project.html, accessed on August 31, 2007.

2.4S.4-4   "Disaster Ready Austin: Building a Safe, Secure and Sustainable Community," City of Austin Hazard Mitigation Action Plan, 2003 – 2008, prepared by LCRA and H2O, Inc., revised on August 7, 2003.

2.4S.4-5   STPEGS Updated Final Safety Analysis Report, Units 1 & 2, Revision 13.

2.4S.4-6   "Water for Texas – 2007," Volumes I, II, and III, Texas Water Development Board, January 2007.

2.4S.4-7   Determining Design Basis Flooding at Power Reactor Sites," La Grange Park, Illinois, ANSI/ANS-2.8-1992, American Nuclear Society, July 1992. (Historical Technical Reference)

2.4S.4-8   "Engineering Data on Dams and Reservoirs in Texas," Part III, Report 126, Texas Water Development Board, February 1971.

2.4S.4-9   "HEC-RAS, River Analysis System, Version 3.1.3," U.S. Army Corps of Engineers, Hydrologic Engineering Center, May 2005.

2.4S.4-10   "Flood Damage Evaluation Project," Chapter 1-6, Volume II-C, Volume II-B, Halff Associates, Inc., July 2002.

2.4S.4-11   "Industries Regulations, Guidelines and Manual – Engineering Guidelines for the Evaluation of Hydropower Projects," Federal Energy Regulatory Commission, April 1991.

2.4S.4-12   D. L. Fread and J. M. Lewis, "NWS FLDWAV Model Theoretical Description and User Documentation," Hydrologic Research Laboratory, Office of Hydrology, National Weather Service, U.S. National Oceanic and Atmospheric Agency, Silver Spring, Maryland, 1998.

2.4S.4-12a   "User's Guide to RMA2 WES," Version 4.5., Coastal and Hydraulics Laboratory, Waterways Experiment Station, Engineer Research and Development Center, U.S. Army Corps of Engineers, April 22, 2005.

2.4S.4-12b   Not Used

2.4S.4-12c   Surface-water Modeling System (SMS), Version 10.0.7, Aquaveo, August 29, 2008.

2.4S.4-12d   T. L. Wahl, "Prediction of Embankment Dam Breach Parameters, A Literature Review and Needs Assessment", Dam Safety Research Report DSO-98-004, Dam Safety Office, Water Resources Research Laboratory, U.S. Department of the Interior, Bureau of Reclamation, July 1998.

2.4S.4-12e   "Guidelines for Defining Inundated Areas Downstream from Bureau of Reclamation Dams," Reclamation Planning Instruction No. 82-11, Dam Safety Office, U.S. Department of Interior, Bureau of Reclamation, Denver, Colorado, 1982.

2.4S.4-12e1 Fread, D. L., BREACH, "An Erosion Model for Earthen Dam Failures", Hydrologic Research Laboratory, Office of Hydrology, National Weather Service, U.S. National Oceanic and Atmospheric Agency, Silver Spring, Maryland, July, 1988.

2.4S.4-12e2 Chow, Ven te, Open Channel Hydraulics, McGraw-Hill Book Company, 1959.

2.4S.4-12e3 Ettema, R. Hydraulic modeling: concepts and practice. Environmental and Water Resources Institute (U.S.). ASCE Publications. 390 pages, 2000.

2.4S.4-12e4 Hughes, S.A. 1993. Physical Models and laboratory techniques in coastal engineering. USACE. ERDC.

2.4S.4-12e5 Su, Y.C., E. Lehotsky, and D. Fuller. 2009. "The Sabine Pass LNG
             Terminal, Challenges for a new LNG Terminal in Louisiana", Caring for
             the Coast: Texas Coastal Conference 2009, Galveston, Texas, June 4-5,
             2009.

2.4S.4-12e6 Su, Y.C. and J. Mahmoud. 2007. Beneficial use of dredged materials at
             Louisiana shoreline near Sabine Pass. International Erosion Control
             Association Conference, Reno NV.

2.4S.4-12e7 Su, Y.C., J. Koutny, J. Benoliel, J. Mahmoud, M. Heaney, and D.
             Granger. 2005. "Sediment Transport Modeling of Dredged Disposal
             Materials Near Sabine Pass." Coastal Texas 2020 Technical Erosion
             Conference 2005, Houston, Texas, September 14-16, 2005.

2.4S.4-12e8 Su, Y.C., C. Woodward, J. Koutny, and J. Benoliel, and W. Crull. 2004.
             "Modeling of Flood Control Channels Using SMS/RMA2." TFMA 17th
             Annual Texas Flood Conference, Fort Worth, Texas, 2004.

2.4S.4-12f   G. J. Arcement and V. R. Schneider, "Guide for Selecting Manning's
             Roughness Coefficients for Natural Channels and Flood Plains,"
             Water-Supply Paper 2239, United States Geological Survey, 1989.

2.4S.4-12g   "Flood Damage Evaluation Project," Chapter 1-6, Volume II-C, Volume
             II-B, Hall Associates, Inc., July 2002.

2.4S.4-12h   "HEC-RAS, River Analysis System, User's Manual," Version 3.1.3, U.S.
             Army Corps of Engineers, Hydrologic Engineering Center, May 2005.

2.4S.4-12i   Z. Xiuzhong and W. Guangqian, "Flow Analysis and Scour Hole
             Computation of Dyke-Breach.," Proceedings of the International
             Association for Hydraulic Researchers XXIX Congress, Theme E,
             Tsinghua University, Beijing, China, September 16-21, 2001.

2.4S.4-13   "Coastal Engineering Manual," U.S. Army Corps of Engineers, June
             2006.

2.4S.4-14   "Advanced Series on Ocean Engineering, Volume 16, Introduction to
             Coastal Engineering and Management," J. William Kamphuis, 2000.

2.4S.4-15   "Colorado River – Flood Guide," Lower Colorado River Authority, Texas,
             January 2003.

Table 2.4S.4-1 Summary of the 68 Dams in Colorado River Basin with 5,000 AF or More Storage Capacity

No.	Dam Name	County	Height of Dam (ft)	Length of Dam (ft)	Top of Dam Elevation (ft MSL)	Maximum Capacity (AF at top of dam)	Dam Type	Date of Completion
01	Mansfield Dam	Travis	266.4	7,089	750.1 (754.1 ft: top of parapet)	3,300,000 [4]	Concrete Gravity Earth and Rockfill	1942
02	Simon Freese Dam [5]	Coleman	148	15,950	1584	1,470,000 [4]	Earth and Rock Fill Embankment	1990
03	Twin Buttes Dam [5]	Tom Green	134	42,460	1991	1,294,000 [3]	Earthfill	1963
04	Buchanan Dam	Burnet	145.5	10,987	1025.35	1,180,000 [1]	Multiple Concrete Arch, Gated and Gravity sections	1937
05	Robert Lee Dam [5]	Coke	140	21,500	1928	1,074,000 [3]	Earthfill	1969
06	O C Fisher Dam [5]	Tom Green	128	40,885	1964	815,000 [2]	Earthfill	1952
07	Brownwood Dam [5]	Brown	120	1,580	1449.5	448,2000 [1]	Earthfill	1933
08	Lake J B Thomas Dam [5]	Scurry	105	14,500	2280	431,000 [2]	Earthfill	1952
09	Alvin Wirtz Dam	Burnet	118.29	5,491	835.25	226,000 [4]	Concrete and Earthfill	1951
10	Brady Dam [5]	McCulloch	104	8,400	1783	213,000 [3]	Earthfill	1963
11	Natural Dam [1] [5]	Howard	47	[6]	[6]	207,265	Earth	1989
12	Tom Miller Dam	Travis	85	1,590	519	115,404 [1]	Concrete Gravity	1939
13	Coleman Dam [5]	Coleman	90	3,200	1740	108,000 [3]	Earthfill	1966
14	Champion Creek Dam [5]	Mitchell	114	6,800	2109	103,600 [3]	Earthfill	1959
15	Cedar Creek Dam	Fayette	96	8,000	401	101,000 [4]	Earthfill	1977
16	Oak Creek Dam [5]	Coke	95	3,800	2104	83,800 [3]	Earthfill	1952
17	Colorado City Dam [5]	Mitchell	85	4,800	2090	78,400 [4]	Earthfill	1949
18	Hords Creek Dam [5]	Coleman	91	6,800	1939	66,300 [3]	Earthfill	1948
19	Roy Inks Dam	Burnet	96.5	1,547.5	922	63,500 [1]	Concrete Gravity	1938

Table 2.4S.4-1 Summary of the 68 Dams in Colorado River Basin with 5,000 AF or More Storage Capacity (Continued)

No.	Dam Name	County	Height of Dam (ft)	Length of Dam (ft)	Top of Dam Elevation (ft MSL)	Maximum Capacity (AF at top of dam)	Dam Type	Date of Completion
20	Mitchell County Dam [1] [5]	Mitchell	70	[6]	[6]	50,241	Earth	1991
21	Decker Creek Dam	Travis	83	6,390	563	45,300 [2]	Earthfill	1967
22	Nasworthy Dam [5]	Tom Green	50	5,480	1883.5	43,300 [4]	Earthfill	1930
23	Ballinger Municipal Lake Dam [1] [5]	Runnels	76	6,200	1,694	34,353	Earth	1985
24	Elm Creek Dam [1] [5]	Runnels	57	5,640	1,810	33,500	Earth	1983
25	Bastrop Dam	Bastrop	85	4,000	458	24,200 [1]	Earthfill	1964
26	Sulphur Springs Draw Dam [1] [5]	Travis	33	[6]	[6]	20,692	Earth	1993
27	Upper Pecan Bayou WS SCS Site 7 Dam [5]	Callahan	63	3,950	1888.9	20,000 [3]	Earthfill	1970
28	Brady Creek WS SCS Site 17 Dam [1] [5]	Mcculloch	50	4,208	[6]	13,511	Earth	1962
29	Brady Creek WS SCS Site 28 Dam [1] [5]	Concho	42	6,459	[6]	13,042	Earth	1957
30	Brady Creek WS SCS Site 31 Dam [1] [5]	Concho	50	5,910	[6]	11,155	Earth	1958
31	Old Lake Winters City Dam [1] [5]	Runnels	37	3,090	1800.2	10,032	Earth	1945
32	Eagle Lake Dam [2]	Colorado	Varies 6 ft +/-	5,300	Not known	9,600 at EL 170 ft, msl	Earthfill	1990
33	Brady Creek WS SCS Site 20 Dam [1] [5]	Concho	43	4,010	[6]	9,494	Earth	1959
34	Northwest Laterals WS SCS Site 5A Dam [1] [5]	Coleman	57	2,631	[6]	9,416	Earth	1971

Table 2.4S.4-1 Summary of the 68 Dams in Colorado River Basin with 5,000 AF or More Storage Capacity (Continued)

No.	Dam Name	County	Height of Dam (ft)	Length of Dam (ft)	Top of Dam Elevation (ft MSL)	Maximum Capacity (AF at top of dam)	Dam Type	Date of Completion
35	Max Starcke Dam	Burnet	98.8	860	766 [1] 738 [7]	8,760 [1]	Concrete with Roof-weir Gated	1951
36	Jim Ned Creek WS SCS Site 25 Dam [1] [5]	Coleman	44	2,400	[6]	8,368	Earth	1963
37	Jim Ned Creek WS SCS Site 12E1 Dam [1] [5]	Coleman	64	2,000	[6]	8,271	Earth	1965
38	Ballinger City Lake Dam [1] [5]	Runnels	30	4,400	1704.6	8,215	Earth	1947
39	Elm Creek WS_NRCS Site 3 Rev. [1] [5]	Runnels	39	[6]	[6]	8,165	Earth	2004
40	Clear Creek WS SCS Site 6 Dam [1] [5]	Brown	50	2,101	1461	8,083	Earth	1958
41	Jim Ned Creek WS SCS Site 21 Dam [1] [5]	Coleman	92	1,915	[6]	7,930	Earth	1963
42	Clear Creek WS SCS Site 4 Dam [1] [5]	Brown	45	2,300	1508.6	7,891	Earth	1958
43	Upper Pecan Bayou WS SCS Site 2 Dam [1] [5]	Callahan	69	2,025	1948.8	7,833	Earth	1967
44	Brady Creek WS SCS Site 14 Dam [1] [5]	Mcculloch	43	4,091	[6]	7,732	Earth	1956
45	Home Creek WS SCS Site 13 Dam [1] [5]	Coleman	45	2,410	[6]	7,679	Earth	1974
46	Valley Creek WS SCS Site 1 Dam [1] [5]	Nolan	52	5,100	2121.8	7,600	Earth	1968
47	Upper Pecan Bayou WS SCS Site 24 Dam [1] [5]	Coleman	50	1,800	1606.4	7,394	Earth	1972

Table 2.4S.4-1 Summary of the 68 Dams in Colorado River Basin with 5,000 AF or More Storage Capacity (Continued)

No.	Dam Name	County	Height of Dam (ft)	Length of Dam (ft)	Top of Dam Elevation (ft MSL)	Maximum Capacity (AF at top of dam)	Dam Type	Date of Completion
48	Brownwood Laterals WS SCS Site 3 Dam [1] [5]	Brown	83	1,930	1473.9	7,377	Earth	1973
49	Northwest Laterals WS SCS Site 1 Dam [1] [5]	Runnels	50	2,520	[6]	7,181	Earth	1964
50	Brady Creek WS SCS Site 32 Dam [1] [5]	Concho	32	8,075	[6]	7,053	Earth	1959
51	Longhorn Dam [1]	Travis	65	1,240	464	6,850	Earth, Gravity	1960
52	Jim Ned Creek WS SCS Site 23 Dam [1] [5]	Coleman	62	1,980	[6]	6,754	Earth	1962
53	Elm Creek WS NRCS Site 7 [1] [5]	Runnels	39.5	[6]	[6]	6,500	Earth	1998
54	Home Creek WS SCS Site 7A Dam [1] [5]	Coleman	48	3,396	[6]	6,367	Earth	1970
55	Jim Ned Creek WS SCS Site 12 Dam [1] [5]	Coleman	84	1,900	[6]	6,334	Earth	1963
56	Mukewater Creek WS SCS Site 10A Dam [1] [5]	Coleman	35	3,190	1485.7	6,130	Earth	1965
57	Elm Creek Lake Dam [1] [5]	Runnels	23	450	1635	6,018	Earth	1930
58	Clear Creek WS SCS Site 3 Dam [1] [5]	Brown	55	1,950	1451.5	5,988	Earth	1960
59	Se Laterals WS SCS Site 7 Dam [1] [5]	San Saba	43	2,225	[6]	5,899	Earth	1968
60	Brady Creek WS SCS Site 21 Dam [1] [5]	Concho	30	3,543	[6]	5,742	Earth	1958
61	Upper Pecan Bayou WS SCS Site 12 Dam [1] [5]	Callahan	65	1,400	1759.3	5,707	Earth	1967

Table 2.4S.4-1 Summary of the 68 Dams in Colorado River Basin with 5,000 AF or More Storage Capacity (Continued)

No.	Dam Name	County	Height of Dam (ft)	Length of Dam (ft)	Top of Dam Elevation (ft MSL)	Maximum Capacity (AF at top of dam)	Dam Type	Date of Completion
62	Moss Creek Lake Dam [1] [5]	Howard	67	2,450	2341.6	5,700	Earth	1939
63	Cummins Creek WS SCS Site 1 Dam [1]	Lee	25	4,050	450.9	5,627	Earth	1958
64	Brady Creek WS SCS Site 36 Dam [1] [5]	Concho	33	1,973	[6]	5,352	Earth	1955
65	Northwest Laterals WS SCS Site 2 Dam [1] [5]	Coleman	52	2,082	[6]	5,297	Earth	1964
66	Jim Ned Creek WS SCS Site 26A Dam [1] [5]	Coleman	46	4,000	[6]	5,280	Earth	1966
67	Jim Ned Creek WS SCS Site 19 Dam [1] [5]	Taylor	28	2,985	[6]	5,218	Earth	1960
68	Clear Creek WS SCS Site 1 Dam [1] [5]	Brown	40	1,542	1397.6	5,128	Earth	1960

[1]   Data provided by TCEQ
[2]   Data provided by TWDB: data was directly listed in Reference 2.4S.4-8
[3]   Data provided by TWDB: data were extrapolated based on the storage-stage curves in Reference 2.4S.4-8
[4]   Data provided by TWDB: data were extrapolated based on the storage-stage area data
[5]   Dams located upstream of Buchanan Dam
[6]   No information was given by TCEQ
[7]   Data from LCRA in Reference 2.4S.4-15

Table 2.4S.4-2 500-year and SPF Inflow Peak Discharges at Selected Locations along the Colorado River (in cfs)

Flood Event	Buchanan	Mansfield	Tom Miller	Bastrop	Garwood	Wharton	Bay City
500-year	382,400	499,700	366,900	321,900	256,700	204,700	187,900
SPF	484,800	737,000	402,500	359,900	285,500	237,800	214,200

Source: Reference 2.4S.4-10

Table 2.4S.4-3 Breach Parameters for Buchanan and Mansfield Dams

Breach Parameters	Buchanan Dam	Mansfield Dam
Average Width of Breach (ft)	1470	1360
Breach Bottom Elevation (ft, MSL)	879.8	484
Breach Top Elevation (ft, MSL)	1,028.4	757
Side Slope of Breach	0	0
Breach Time to Failure (hrs)	0.1	0.1

Table 2.4S.4-4 Initial Estimation of Manning's Roughness Coefficient

n Values Assigned to the USGS NLCD Dataset		
USGS Classification Grid-Code	**Description**	***n* Value**
11	Open water	0.03
21	Low intensity residential	0.07
22	High intensity residential	0.09
23	Commercial/industrial/transportation	0.10
31	Bare rock/sand/clay	0.04
32	Quarries/strip mines/gravel pits	0.035
41	Deciduous forest	0.095
42	Evergreen forest	0.085
51	Shrubland	0.08
71	Grasslands/herbaceous	0.04
81	Pasture/hay	0.045
82	Row crops	0.05
83	Small grains	0.055
85	Urban/recreation grasses	0.03
91	Woody wetlands	0.10
92	Emergent herbaceous wetlands	0.085

Source: Reference 2.4S.4-10

Table 2.4S.4-5 MCR Embankment Breach Parameters and Peak Discharge Based on Empirical Equations from Reference 2.4S.4-12d

Parameter	Equation	Results
(1) Time to Failure (hrs)	$t_f = 0.0179(0.0261(V*h_w)^{0.769})^{0.364}$	1.7 hours
(2) Average Breach Width (m)	$B_{ave} = 0.1803\ V^{0.32}\ h_b^{0.19}$	127 m (417 ft)
(3) Peak Flow (m³/s)	$Q_p = 0.607\ V^{0.295}\ h_w^{1.24}$	1172.8 m³/s (62,600 cfs)
B_{ave} = average breach width h_w = depth of water above breach in m = 50.9' – 29' = 21.9' = 6.7 m h_b = the height of breach from the top of embankment in m = 66' – 29' = 37' = 11.3 m V = volume of water in the MCR between El. 29' and El. 50.9' in m³ = 188,400,000 m³ (152,700 ac-ft) (1) MacDonald and Langridge-Monopolis Time to Failure (2) Froelich's Average Breach Width (3) Froelich's Peak Flow		

Table 2.4S.4-6 MCR Embankment Breach Outflow Hydrograph

Time (hours)	Flow (cfs)	MCR Water Surface Elevation (ft)
0	0	50.90
0.1	1,100	50.90
0.2	3,970	50.89
0.3	8,570	50.88
0.4	15,500	50.87
0.5	24,700	50.85
0.6	30,600	50.82
0.7	37,200	50.78
0.8	47,300	50.73
0.9	54,700	50.68
1.0	79,600	50.59
1.1	85,900	50.49
1.2	92,300	50.40
1.3	100,700	50.28
1.4	108,500	50.15
1.5	116,100	50.03
1.6	123,500	49.88
1.7	130,000	49.74
1.8	126,700	49.58
1.9	124,500	49.46
2.0	122,600	49.29
2.1	120,800	49.13
2.2	119,000	49.00
2.3	117,400	48.86
2.4	115,600	48.70
2.5	113,900	48.56
3	112,800	47.88
6	83,150	44.44
9	63,030	41.86
12	48,890	39.88
15	38,680	38.32
18	31,110	37.08
21	25,390	36.07
24	21,000	35.24
27	17,560	34.56
30	14,840	33.98

Table 2.4S.4-6a Results of Sensitivity Analysis for Breach Parameters Selected for use with FLDWAV

Parameter	Time to Fail t_f (hours)	Percent Difference	Breach Width B (ft)	Percent Difference	Peak Flow Qp (cfs)	Percent Difference
Adopted	1.7		380		130,000	
Increased t_f	1.4	18			132,000	+ 1.5
Decreased t_f	2.0	18			128,200	- 1.1
Increased B			446	18	157,700	+ 21
Decreased B			310	18	104,400	- 20

Table 2.4S.4-6b Comparison of Manning's n-value to BREACH Analysis Results

Manning's Roughness Coefficient (n-value)	Peak Discharge (cfs)	Time to Peak (hrs)	Breach Bottom Width at Peak Flowrate (ft)	Final Breach Bottom Width (ft)	Reservoir Water Level at Time of Peak Flowrate (ft)
0.025	30,760	15.9	132	179	46.4
0.05	83,200	6.25	361	448	46.8
0.08	122,800	2.4	465	619	48.9

Table 2.4S.4-6c Comparison of Results from BREACH and FLDWAV Models

Model	Peak Discharge (cfs)	Time to Peak (hrs)	Breach Bottom Width at Time of Peak Flowrate
FLDWAV	130,100	1.7	380
BREACH	83,200	6.25	361

Table 2.4S.4-7 Material Types and Associated Manning's *n*

Material Type	Manning's *n*
Water	0.030
Short Hard Building	0.100
Soft Building / High Drag	0.085
Vehicle Barrier Walls (VBW)	0.085
Gravel	0.035
Open Space	0.040
Concrete Slab	0.012
Road (Concrete)	0.013
Channel	0.040
Pipeline	0.100
Artificial Sump	0.100

Table 2.4S.4-7a Peak Flood Discharge per Unit Width at Safety-Related SSCs

Location	Water Surface Elevation (ft)	Water Depth (ft)	Peak Velocity (ft/s)	Peak Discharge per Unit Width (cfs/ft)
Unit 4 UHS	38.8	4.8	0.4	1.9
Unit 4 Power Block, South	38.2	3.8	3.8	14.4
Between Unit 3 and Unit 4	37.6	4.25	4.4	18.7

NOTE: The examples above are based on the West Breach simulation.

Table 2.4S.4-8 Estimated Water Levels due to Dam Break, Wind Setup, and Wave Run-up

	Dam Break Water Level (ft MSL)	Wind Setup (ft)	Wave Run-up (ft)	Water Level at STP Site (ft MSL)
Fetch A	28.6	3.9	1.9	34.4

Dam Location Key

1 MANSFIELD DAM
2 SIMON FREESE DAM
3 TWIN BUTTES DAM
4 BUCHANAN DAM
5 ROBERT LEE DAM
6 OC FISHER DAM
7 LAKE BROWNWOOD DAM
8 LAKE JB THOMAS DAM
9 ALVIN WIRTZ DAM
10 BRADY DAM
11 NATURAL DAM
12 TOM MILLER DAM
13 COLEMAN DAM
14 CHAMPION CREEK DAM
15 CEDAR CREEK DAM
16 OAK CREEK DAM
17 LAKE COLORADO CITY DAM
18 HORDS CREEK DAM
19 ROY INKS DAM
20 MITCHELL COUNTY RESERVOIR DAM
21 DECKER CREEK DAM
22 NASWORTHY DAM
23 BALLINGER MUNICIPAL LAKE DAM
24 ELM CREEK DAM
25 LAKE BASTROP DAM
26 SULPHUR SPRINGS DRAW DAM
27 UPPER PECAN BAYOU WS SCS SITE 7 DAM
28 BRADY CREEK WS SCS SITE 17 DAM
29 BRADY CREEK WS SCS SITE 28 DAM
30 BRADY CREEK WS SCS SITE 31 DAM
31 OLD LAKE WINTERS CITY DAM

Legend

⊠	Dam Locations
—	Colorado River Centerline
▭	STP Boundary
▭	County Boundaries

Dam Locations along the Colorado River in Texas
(Capacity Greater than 10,000 AF)

Projection:	**Universal Transverse Mercator**
Zone:	**Zone 14**
Horizontal Datum:	**North American Datum 1927**

Figure 2.4S.4-1a Locations of Dams with Storage Capacity Over 10,000 AF in the Colorado River Basin Upstream of the STP 3 & 4 Site

Dam Location Key

32 EAGLE LAKE DAM
33 BRADY CREEK WS SCS SITE 20 DAM
34 NORTHWEST LATERALS WS SCS SITE 5A DAM
35 MAX STARCKE DAM
36 JIM NED CREEK WS SCS SITE 25 DAM
37 JIM NED CREEK WS SCS SITE 12E1 DAM
38 BALLINGER CITY LAKE DAM
39 ELM CREEK WS NRCS SITE 3 REV
40 CLEAR CREEK WS SCS SITE 6 DAM
41 JIM NED CREEK WS SCS SITE 21 DAM
42 CLEAR CREEK WS SCS SITE 4 DAM
43 UPPER PECAN BAYOU WS SCS SITE 2 DAM
44 BRADY CREEK WS SCS SITE 14 DAM
45 HOME CREEK WS SCS SITE 13 DAM
46 VALLEY CREEK WS SCS SITE 1 DAM
47 UPPER PECAN BAYOU WS SCS SITE 24 DAM
48 BROWNWOOD LATERALS WS SCS SITE 3 DAM
49 NORTHWEST LATERALS WS SCS SITE 1 DAM
50 BRADY CREEK WS SCS SITE 32 DAM
51 LONGHORN DAM
52 JIM NED CREEK WS SCS SITE 23 DAM
53 ELM CREEK WS NRCS SITE 7 REV
54 HOME CREEK WS SCS SITE 7A DAM
55 JIM NED CREEK WS SCS SITE 12 DAM
56 MUKEWATER CREEK WS SCS SITE 10A DAM
57 ELM CREEK LAKE DAM
58 CLEAR CREEK WS SCS SITE 3 DAM
59 SE LATERALS WS SCS SITE 7 DAM
60 BRADY CREEK WS SCS SITE 21 DAM
61 UPPER PECAN BAYOU WS SCS SITE 12 DAM
62 MOSS CREEK LAKE DAM
63 CUMMINS CREEK WS SCS SITE 1 DAM
64 BRADY CREEK WS SCS SITE 36 DAM
65 NORTHWEST LATERALS WS SCS SITE 2 DAM
66 JIM NED CREEK WS SCS SITE 26A DAM
67 JIM NED CREEK WS SCS SITE 19 DAM
68 CLEAR CREEK WS SCS SITE 1 DAM

Dam Locations along the Colorado River in Texas
(Capacity Between 5,000 and 10,000 AF)

Projection:	Universal Transverse Mercator
Zone:	Zone 14
Horizontal Datum:	North American Datum 1927

Figure 2.4S.4-1b Locations of Dams with Storage Capacity of 5,000 AF to 10,000 AF in the Colorado River Basin Upstream of the STP 3 & 4 Site

Figure 2.4S.4-2 Model Cross Section at Buchanan Dam
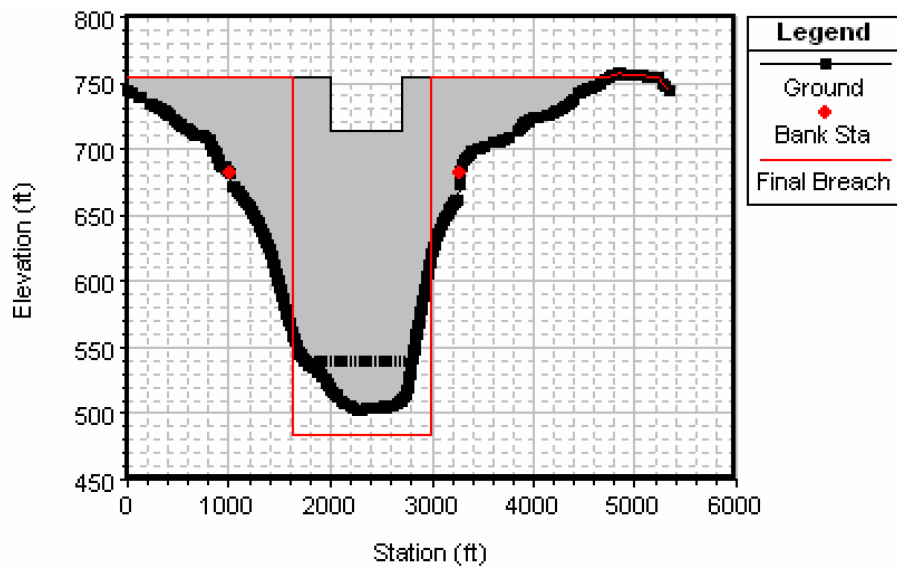
Figure 2.4S.4-3 Model Cross Section at Mansfield Dam
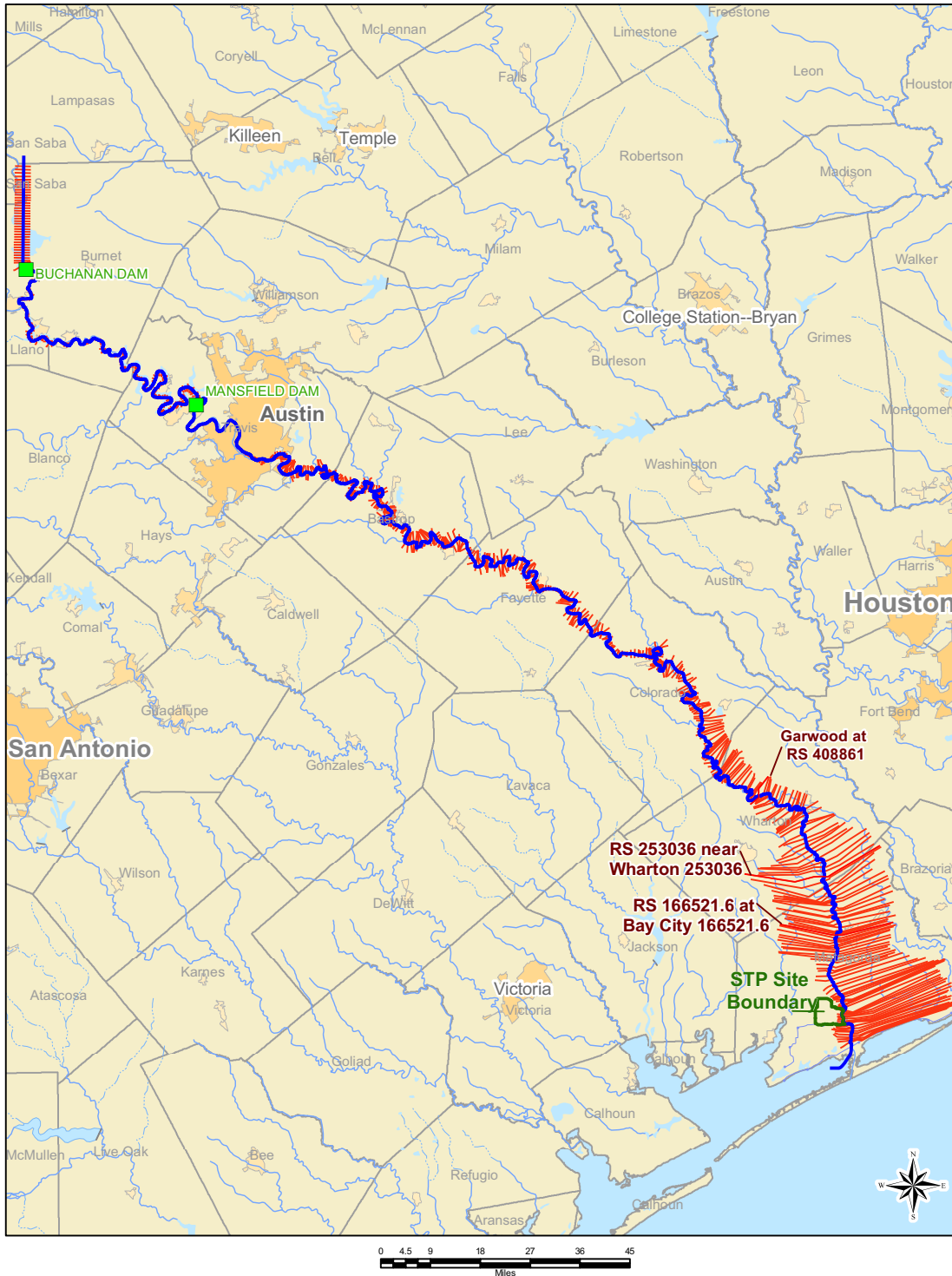
Figure 2.4S.4-4 Locations of Model Cross Sections in the Dam Break Analysis
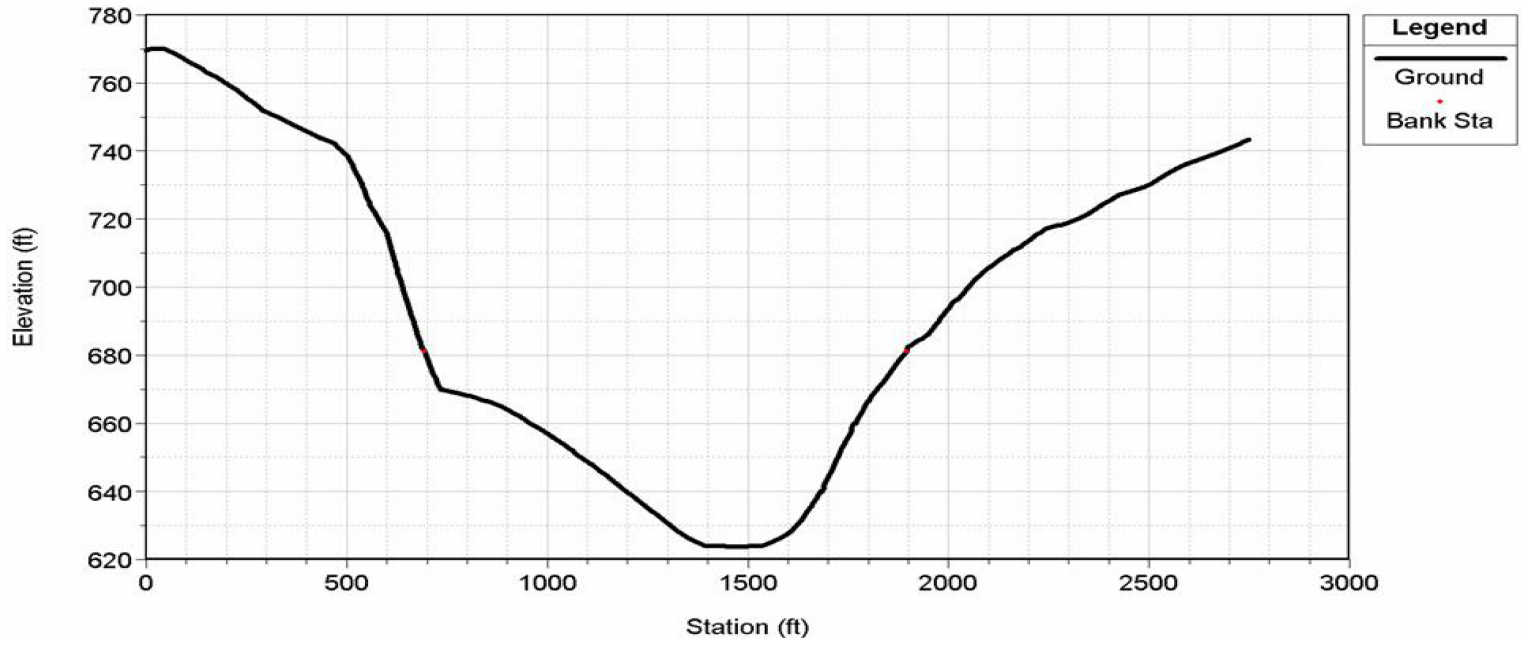
Figure 2.4S.4-5 Model River Cross Section at About 365 River Miles Upstream of the GIWW

Note: Between Buchanan and Mansfield Dams and about 49.6 River Miles Upstream of Mansfield Dam.
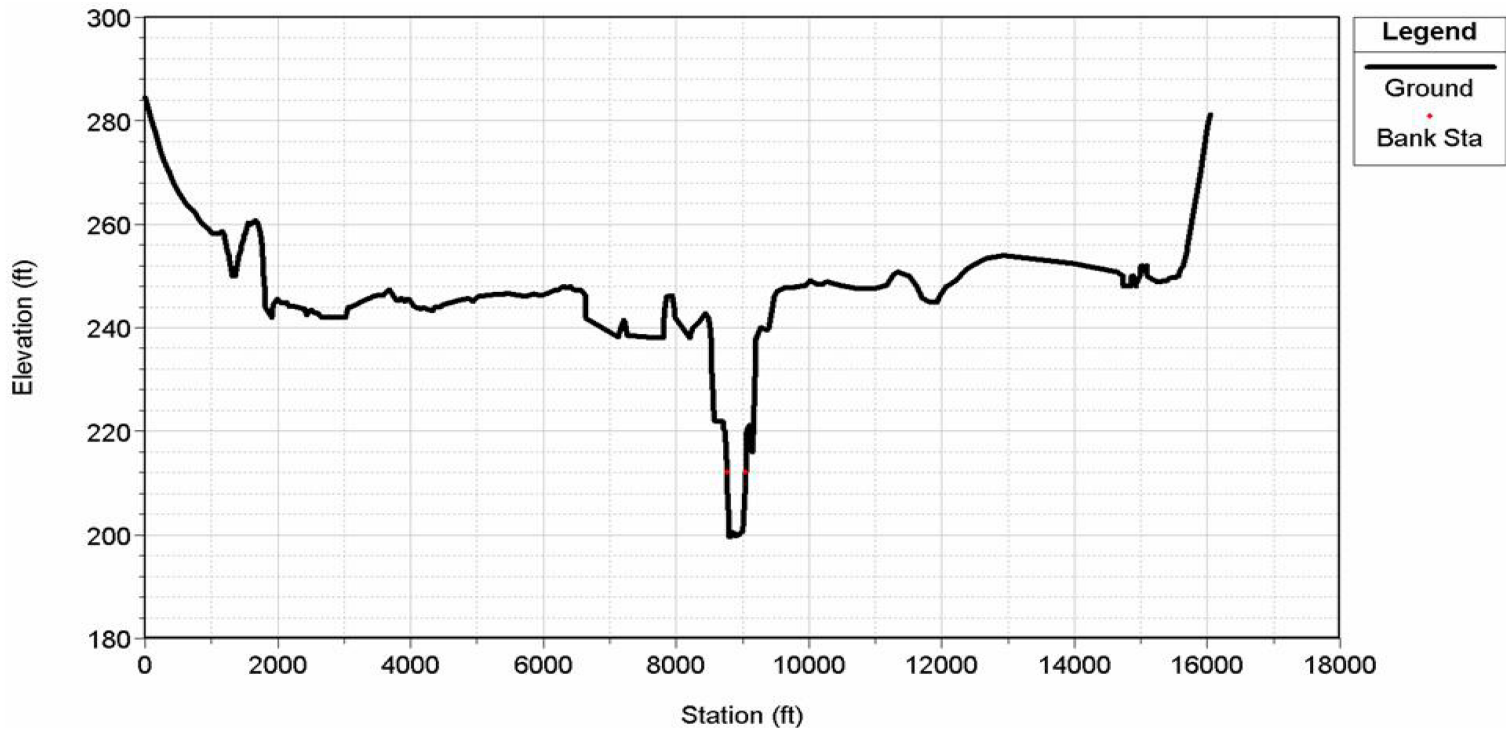
Figure 2.4S.4-6 Model River Cross Section at About 163.5 River Miles Upstream of the GIWW

Note: Downstream of Mansfield Dam and about 153 miles Upstream of STP 3 & 4 Site.
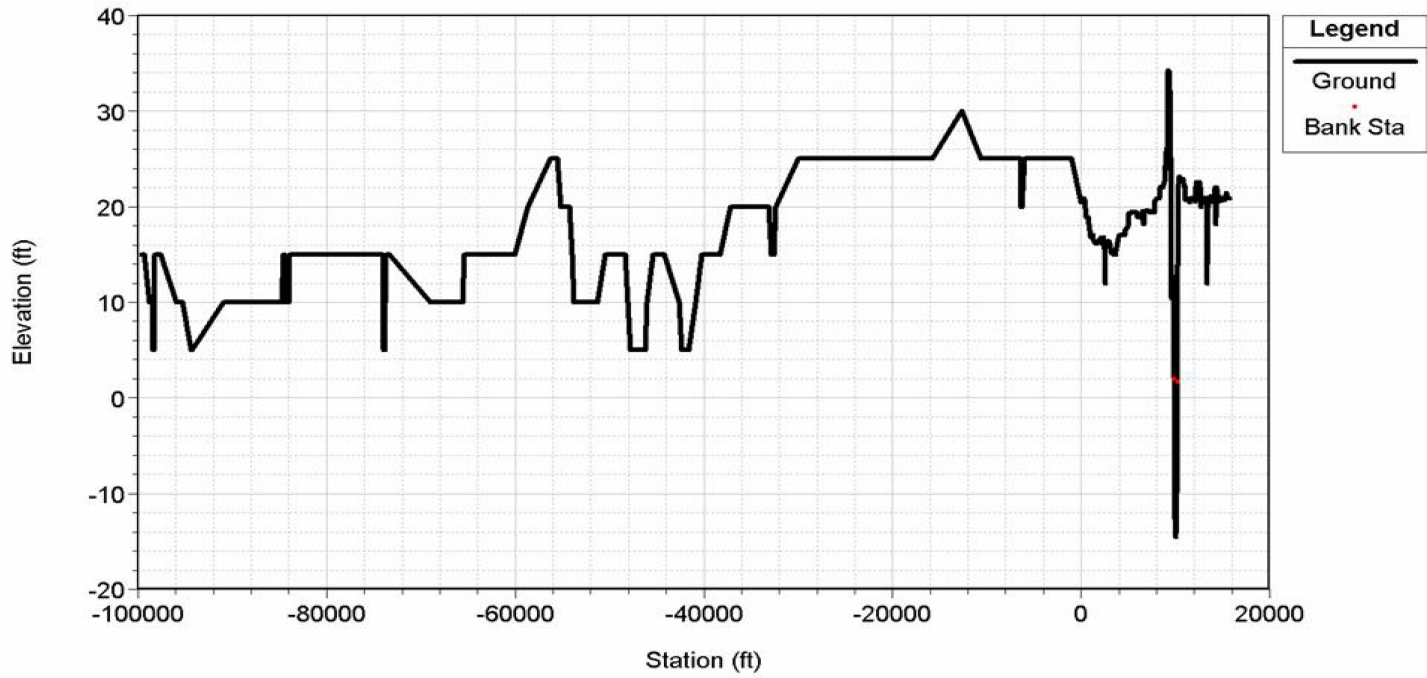
Figure 2.4S.4-7 Model River Cross Section at About 10.5 River Miles Upstream of the GIWW

Note: Near the STP site.
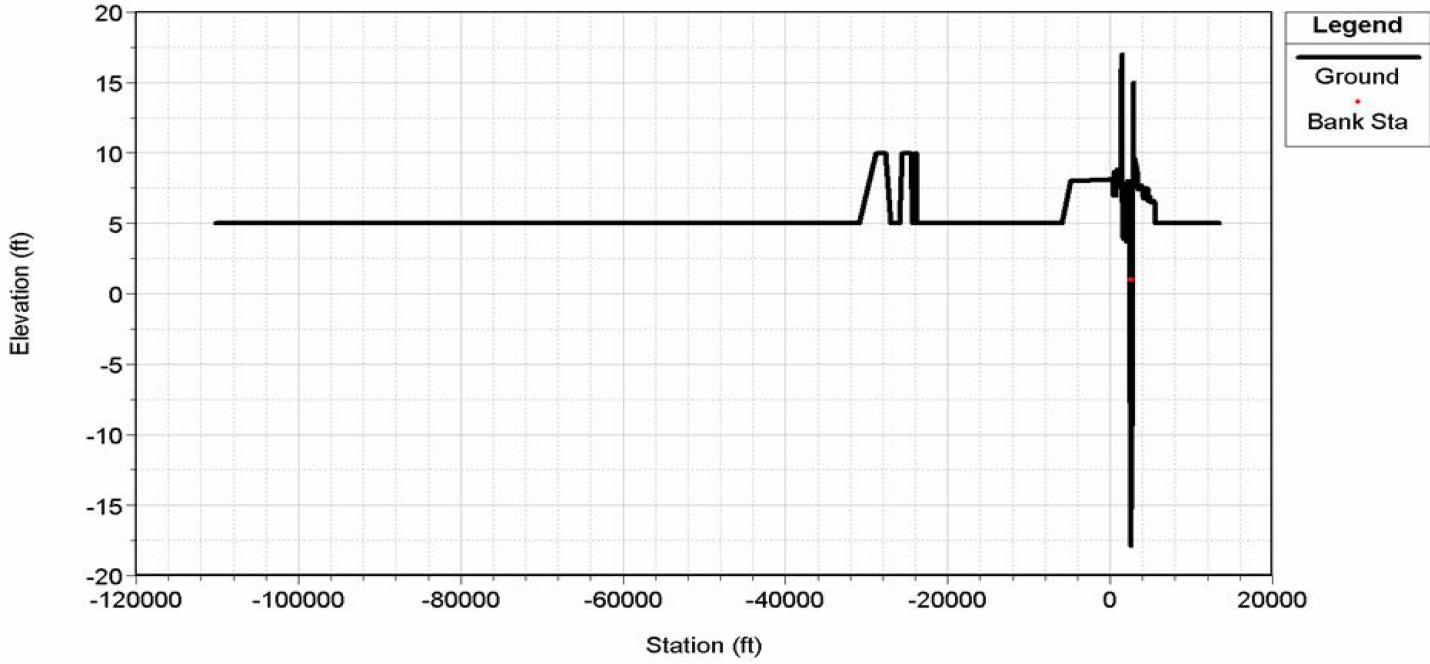
Figure 2.4S.4-8 Model River Cross Section at Downstream Model Boundary at about 0.9 River Miles Upstream of the GIWW

Plan: One n20   River: Colorado   Reach: 1   RS: 89146.04
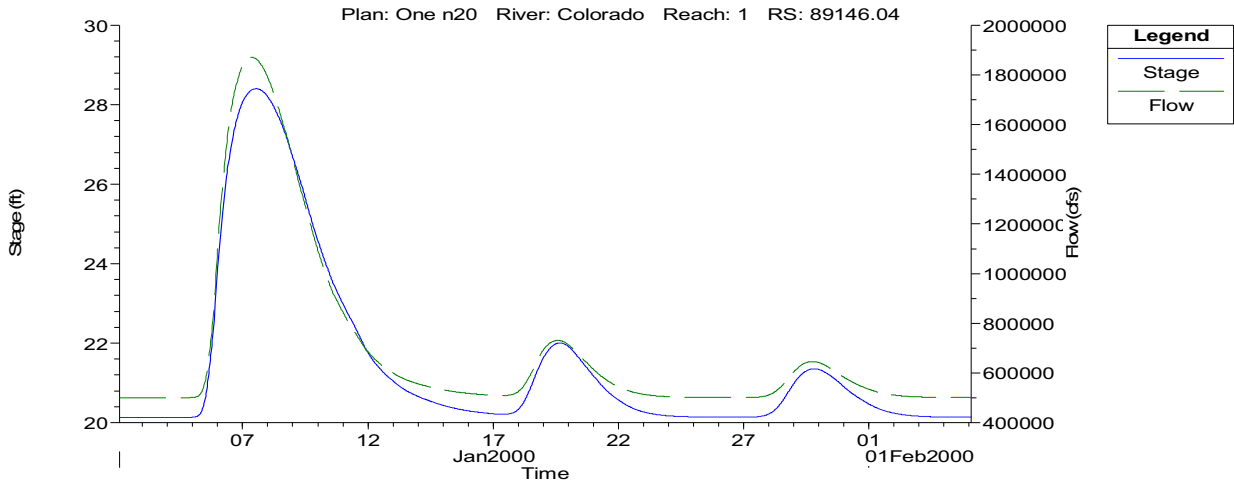
Figure 2.4S.4-9 Based Case Flood and Stage Hydrographs at the STP 3 & 4 Site

Note: Vertical Datum is NAVD 88; model start date was selected arbitrarily.
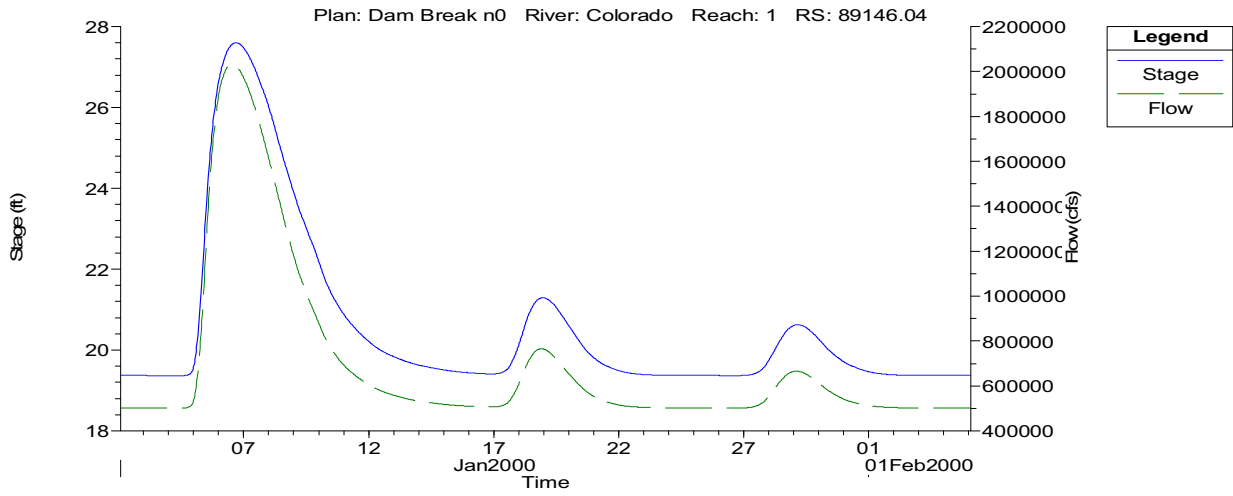
Figure 2.4S.4-10 Sensitivity Case Flood and Stage Hydrographs at the STP 3 & 4 Site

Note: Vertical Datum is NAVD 88; model start date was selected arbitrarily.
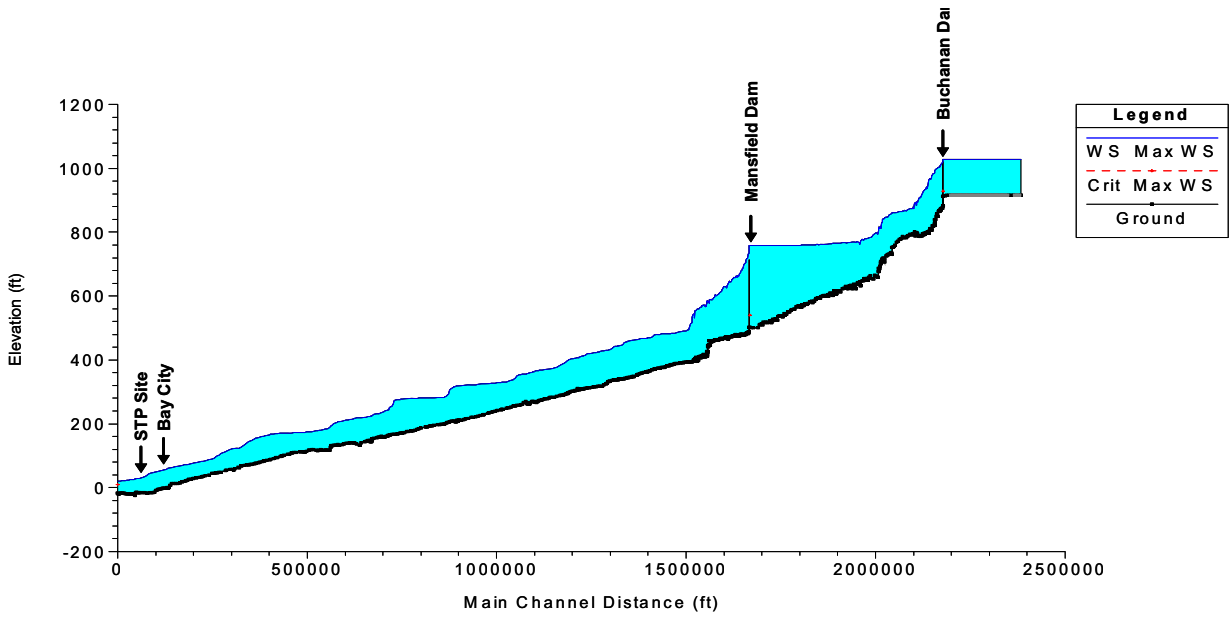
Figure 2.4S.4-11 Base Case Simulated Maximum Dam Break Surface Profiles from Buchanan Dam to 4,600 ft upstream of GIWW (Vertical Datum in NAVD 88)
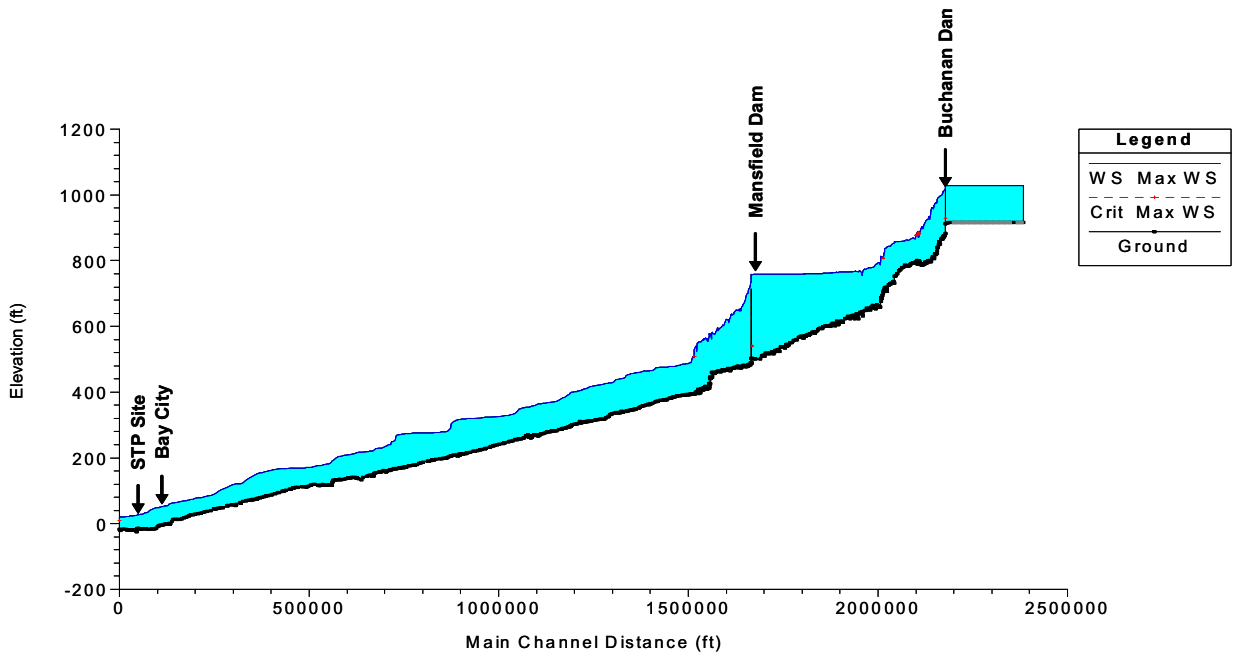
Figure 2.4S.4-12 Sensitivity Case Simulated Maximum Dam Break Surface Profiles from Buchanan Dam to 4600 ft Upstream of GIWW

Note: Vertical Datum in NAVD 88.

EXPERIENCED OUTFLOW RATES FROM BREACHED DAMS

$Q_o = 75(D)^{1.85}$
Q_o = PEAK OUTFLOW IN C.F.S.
D = HYDRAULIC DEPTH IN FT.

MAXIMUM OUTFLOW AT STP

MAXIMUM OUTFLOW FROM HISTORICAL RECORD

HISTORIC FAILURES

NO.	LOCATION
1	SOUTHFORK, JOHNSTOWN, PA.
2	AUSTIN, TX.
3	HATCHTOWN, UT.
4	SCHAEFFER, CO.
5	APISHAPA, CO.
6	FRENCH LANDING, MI.
7	ST. FRANCIS, CA.
8	CASTLEWOOD, CO.
9	OROS, BRAZIL
10	LITTLE DEER CREEK, UT.
11	BALDWIN HILLS, CA.
12	SWIFT, MT.
13	LOWER TWO MEDICINE, MT.
14	HELL HOLE, CA.
15	GRANITE CREEK, AK.
16	BUFFALO CREEK, WV.
17	TETON, ID.
18	SANDY RUN, JOHNSTOWN, PA.
19	LAUREL RUN, JOHNSTOWN, PA.
20	KELLY BARNES, GA.
21	FRED BURR, MT.

Figure 2.4S.4-13 Outflow Rates Experienced from Breached Dams (Reference 2.4S.4-12e)
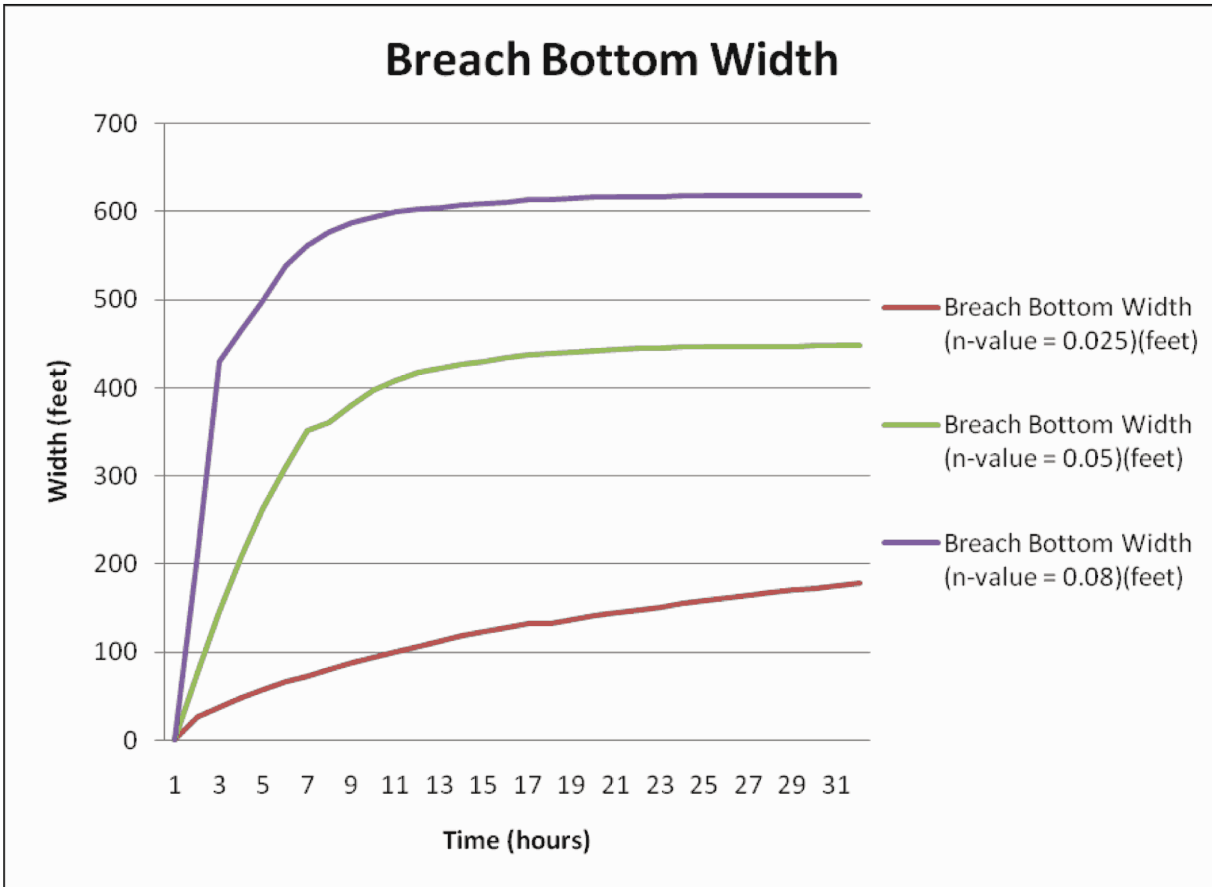
Figure 2.4S.4-13a Breach Width Development for Different n-values
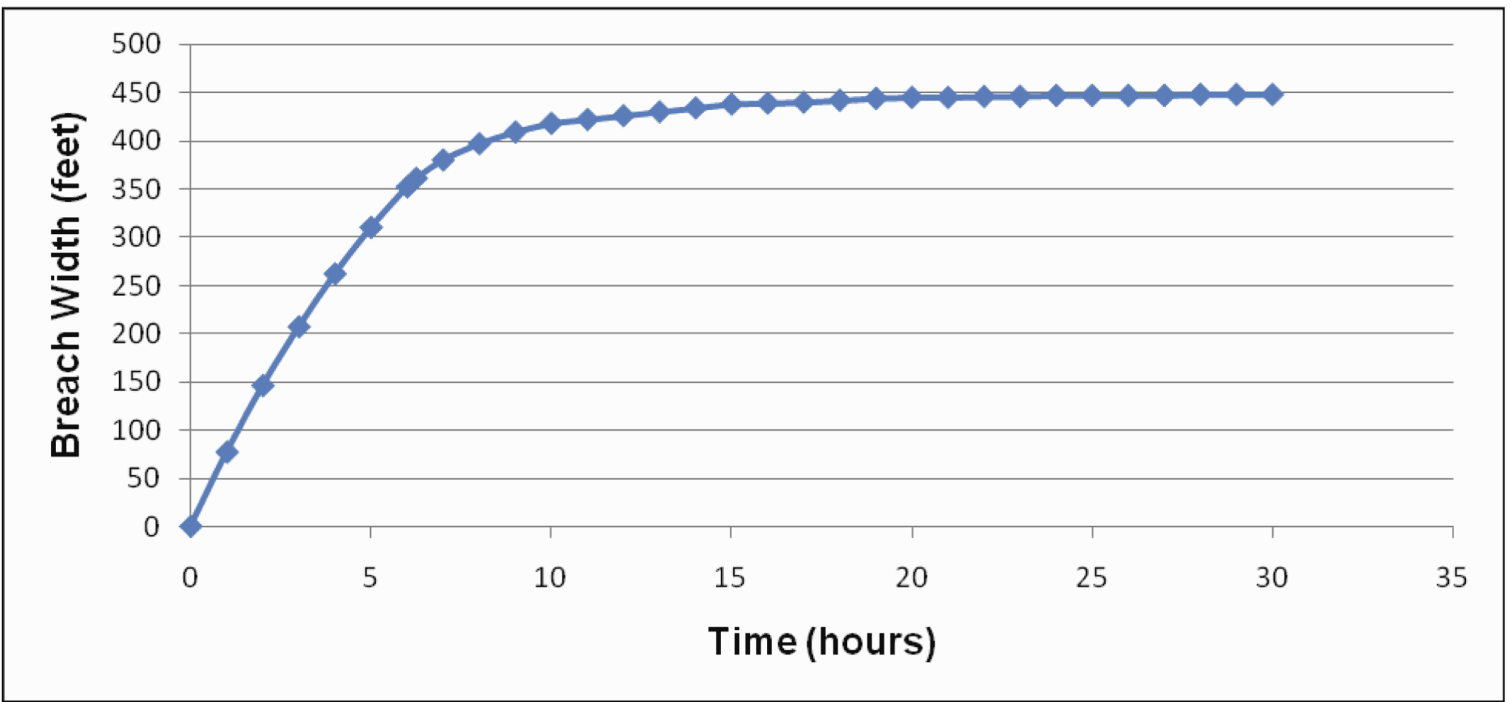
Figure 2.4S.4-13b Breach Bottom Width Development from BREACH analysis
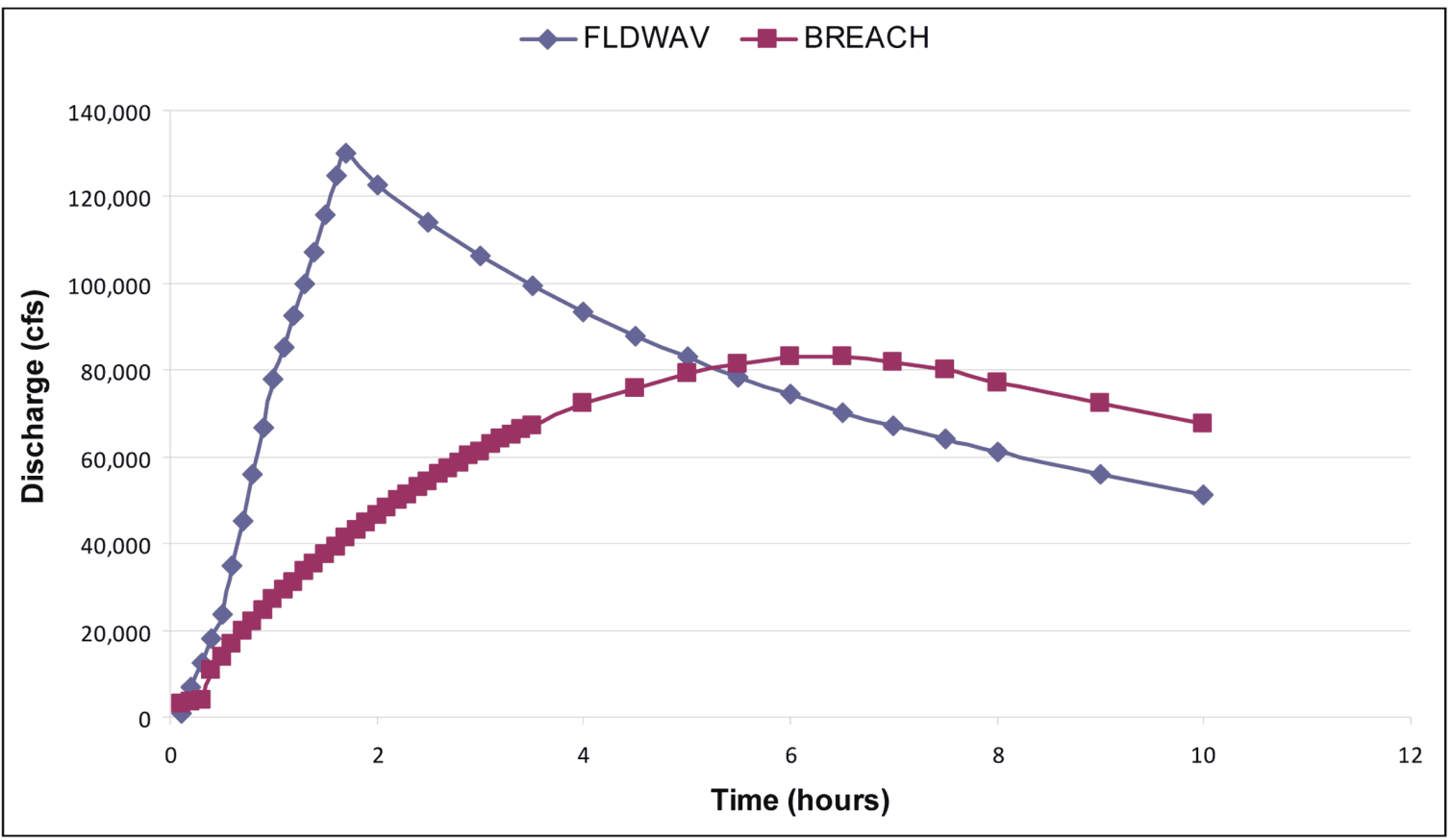
Figure 2.4S.4-13c Comparison of BREACH and FLDWAV Outflow Hydrographs
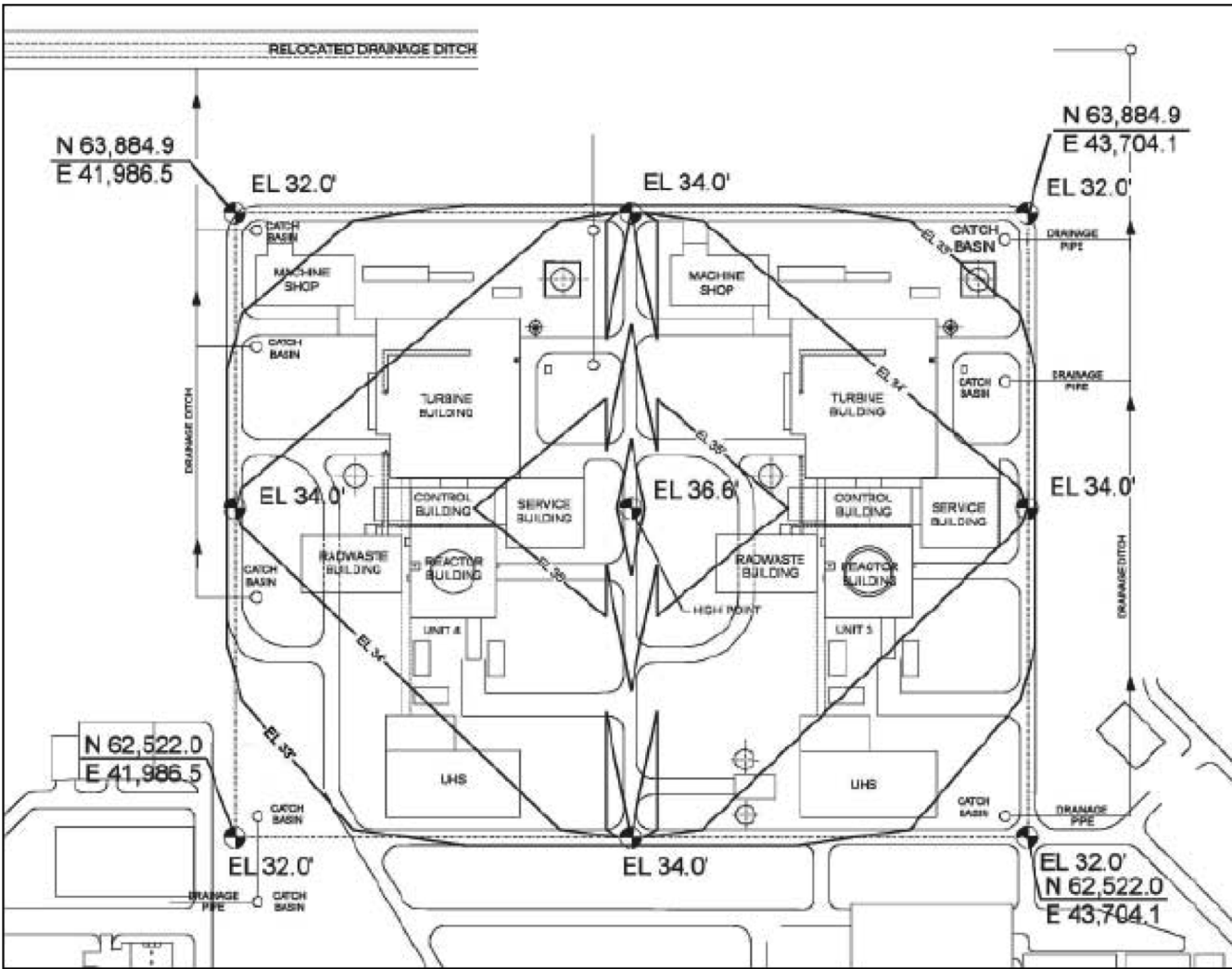
Figure 2.4S.4-14 Units 3 and 4 Site Grading Plan
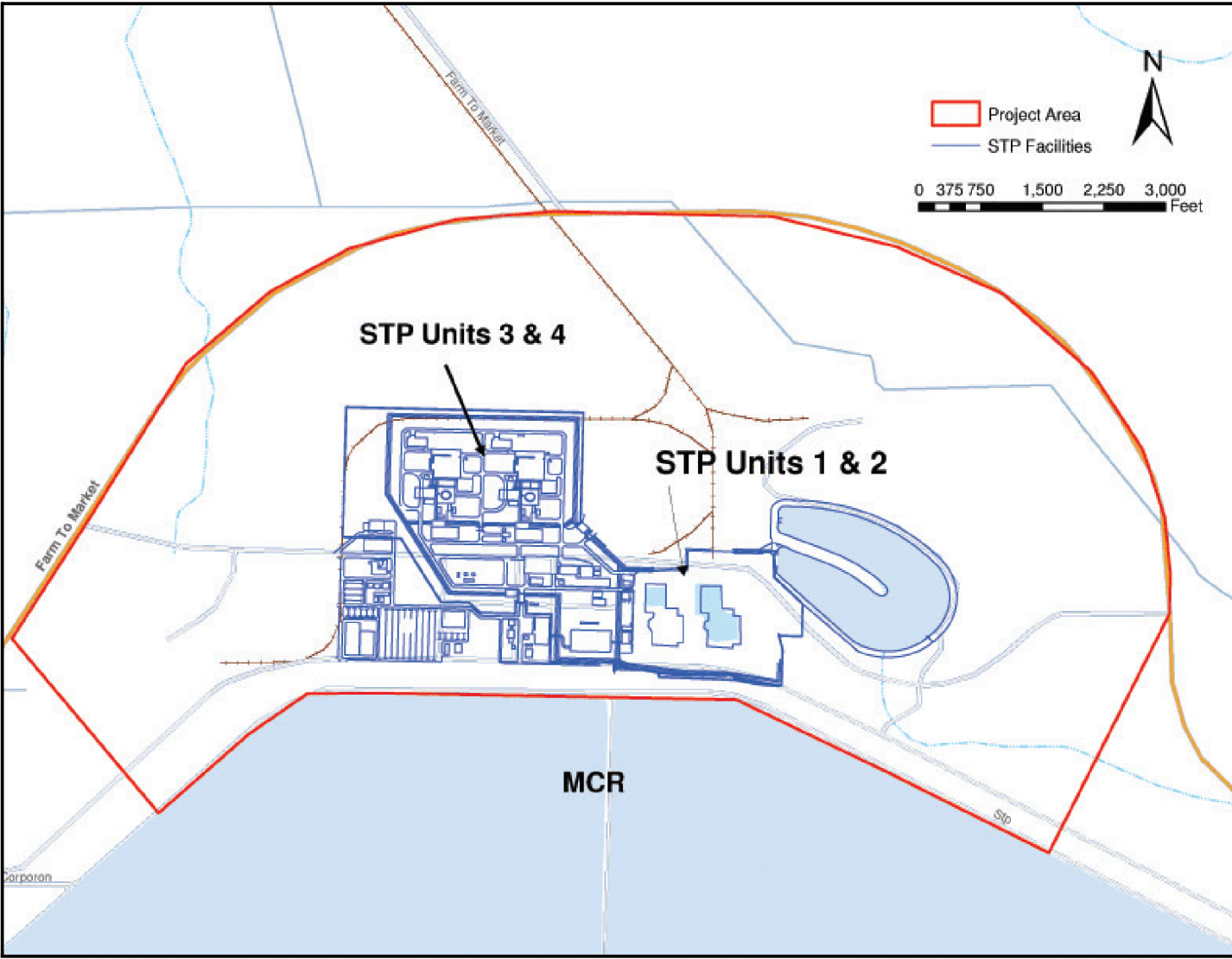
Figure 2.4S.4-15 STP Site Layout
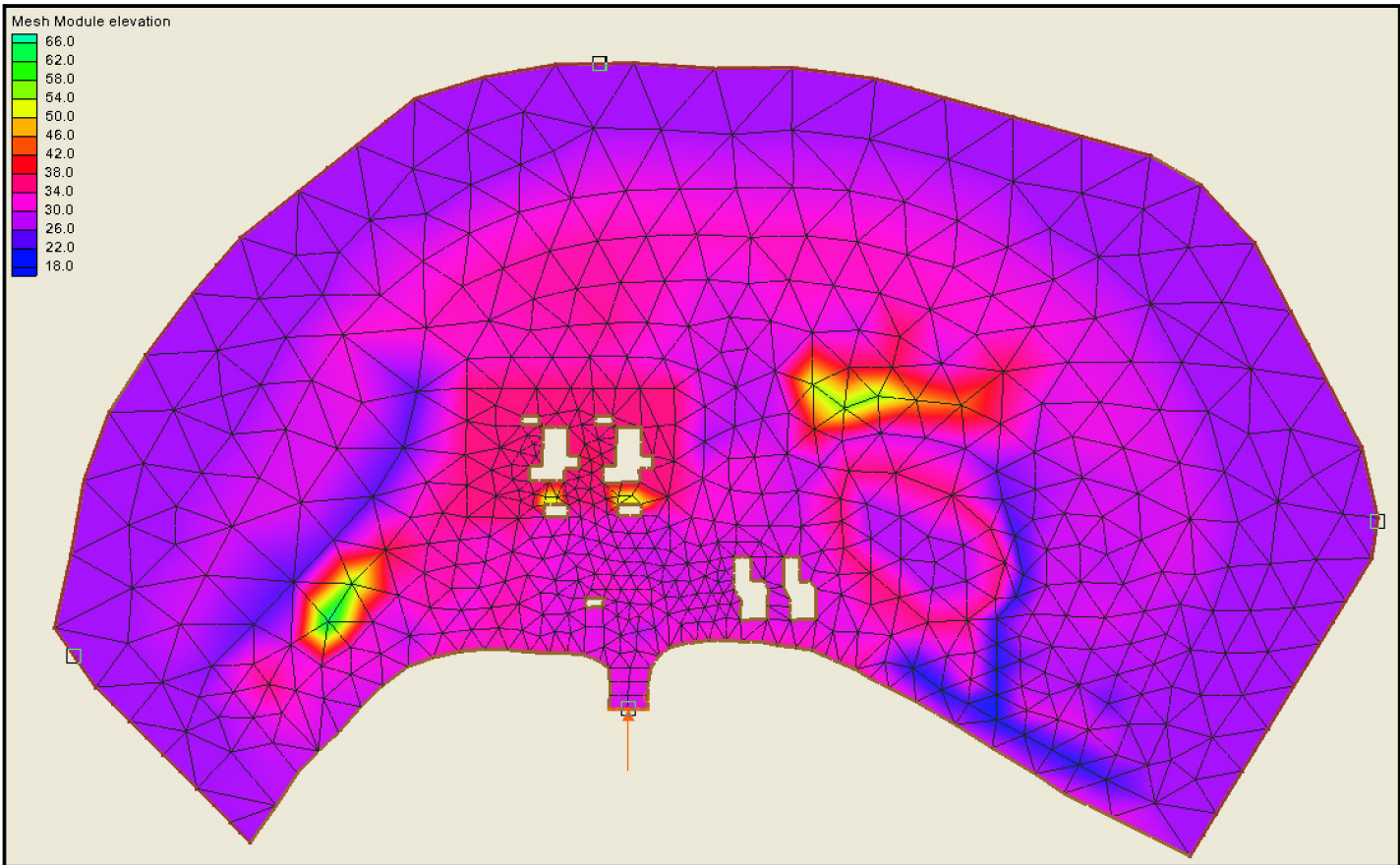
Figure 2.4S.4-16 Two-Dimensional View of Developed 2-D Grid with an East Breach
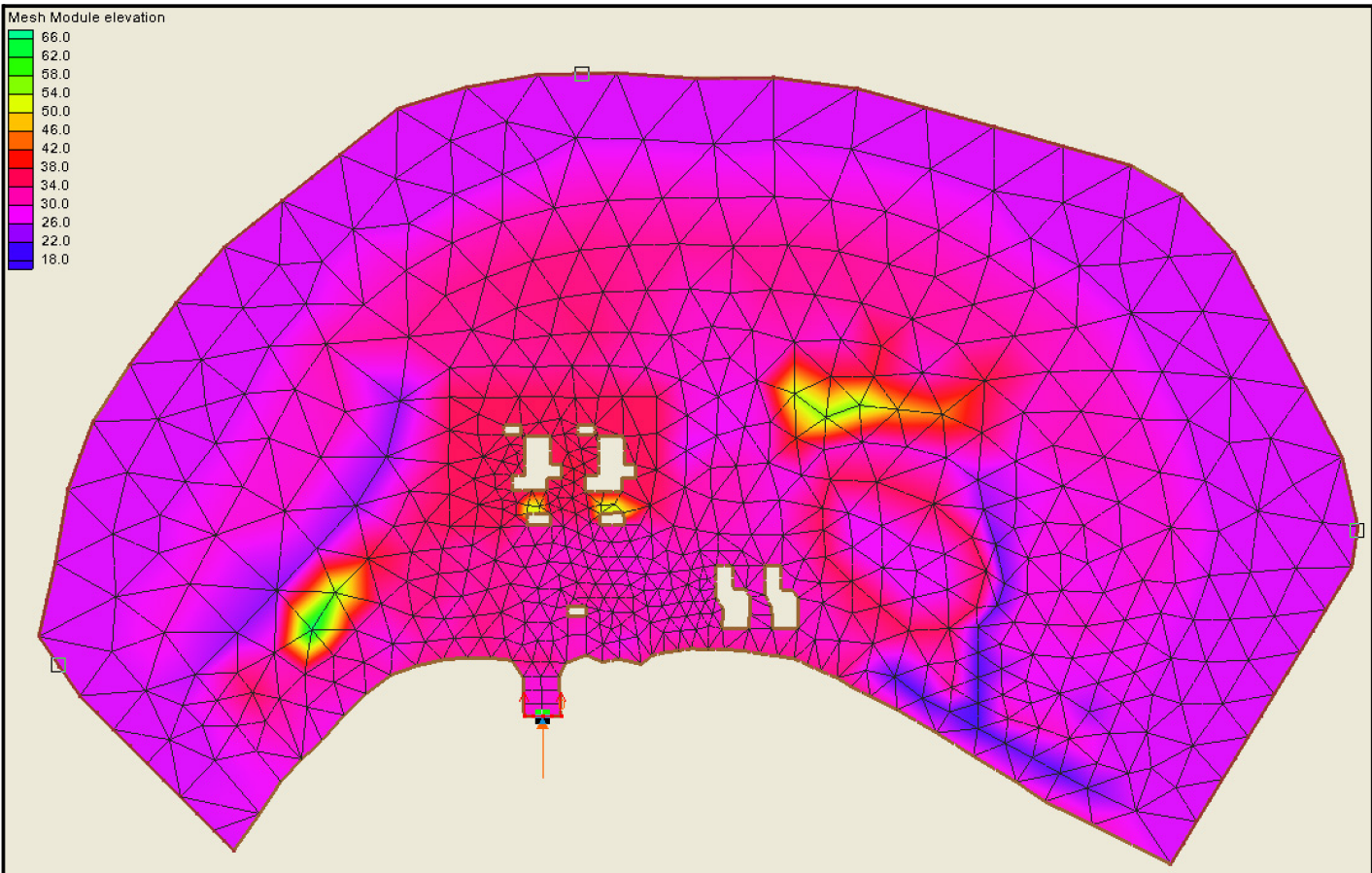
Figure 2.4S.4-17 Two-Dimensional View of Developed 2-D Grid with a West Breach
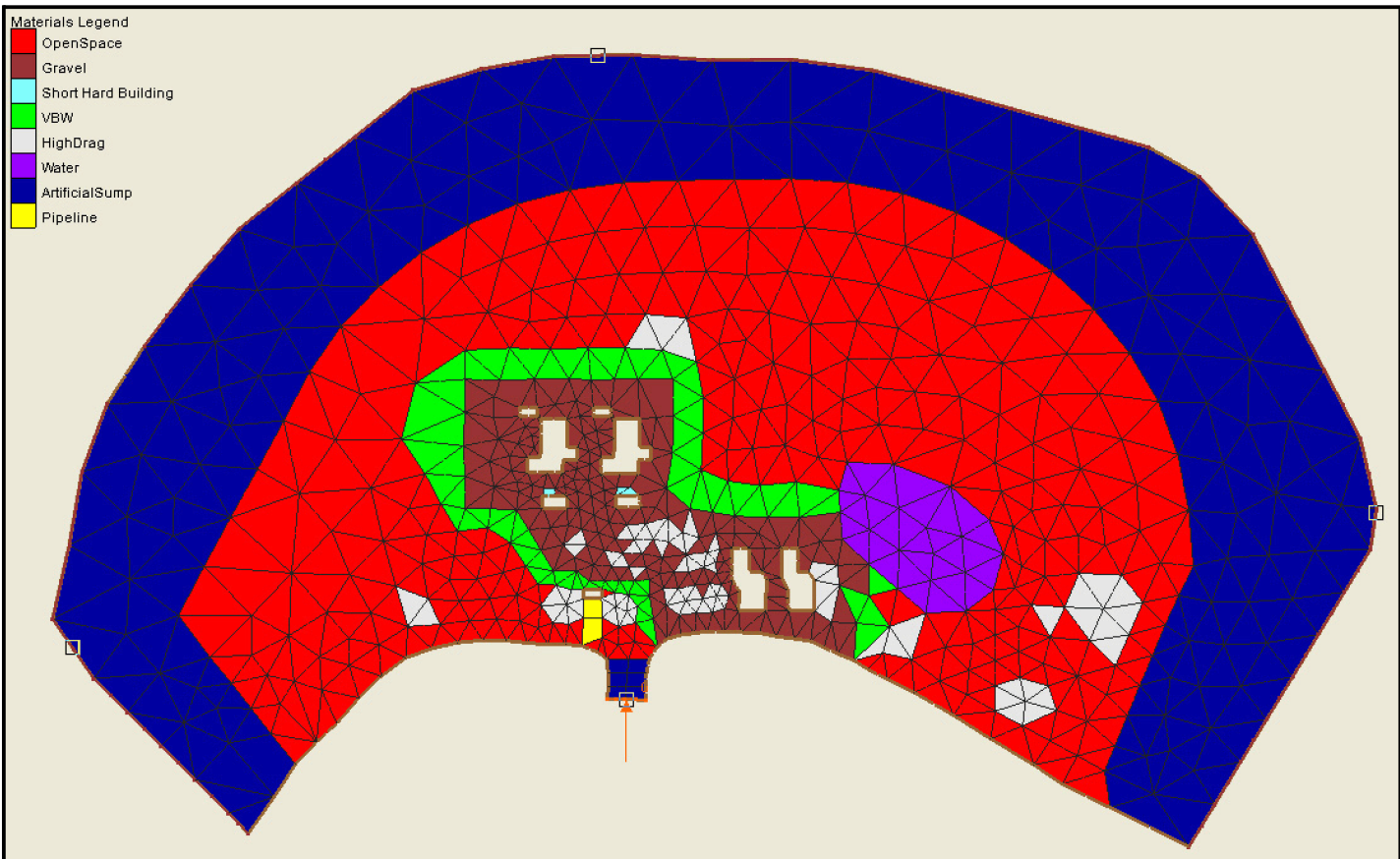
Figure 2.4S.4-18 Assigned Material Types of Developed 2-D Grid
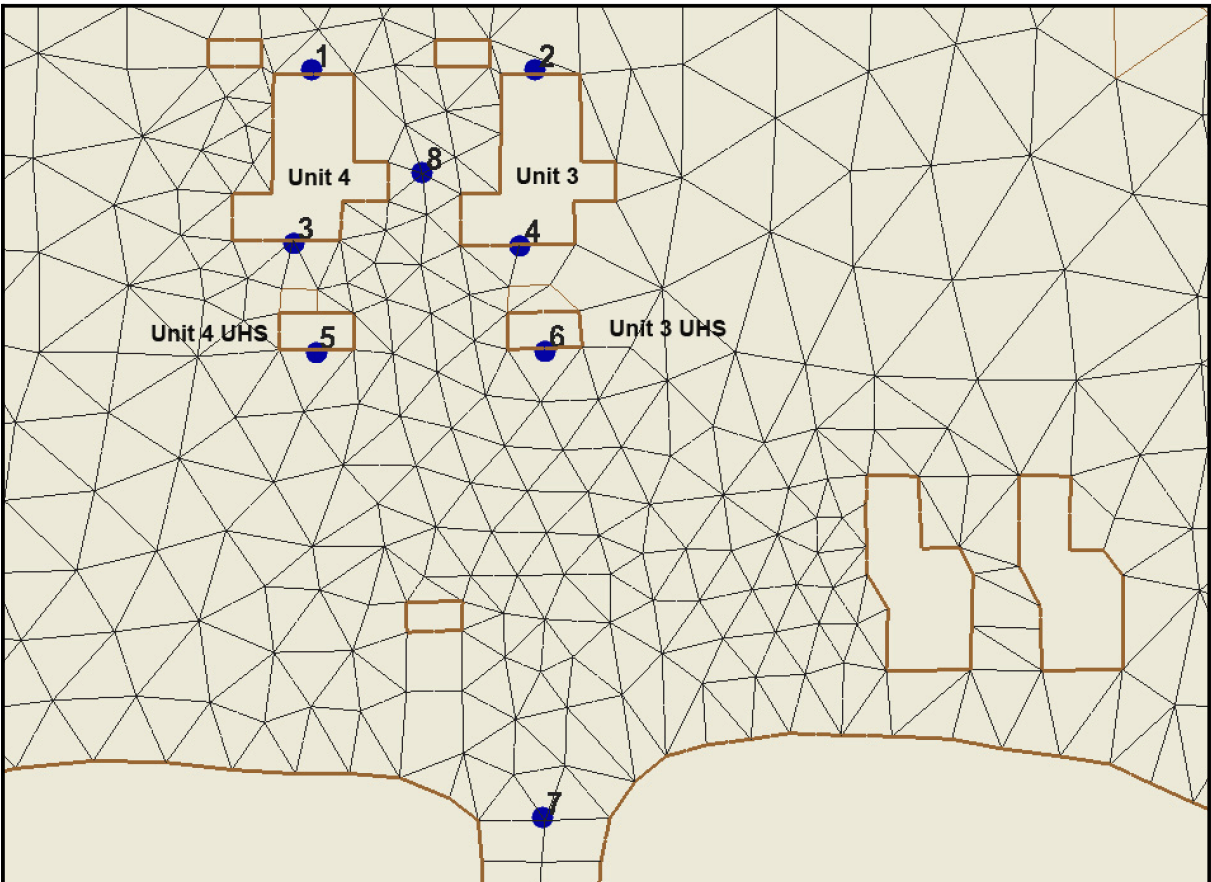
Figure 2.4S.4-19 Locations for RMA2 Modeling Results
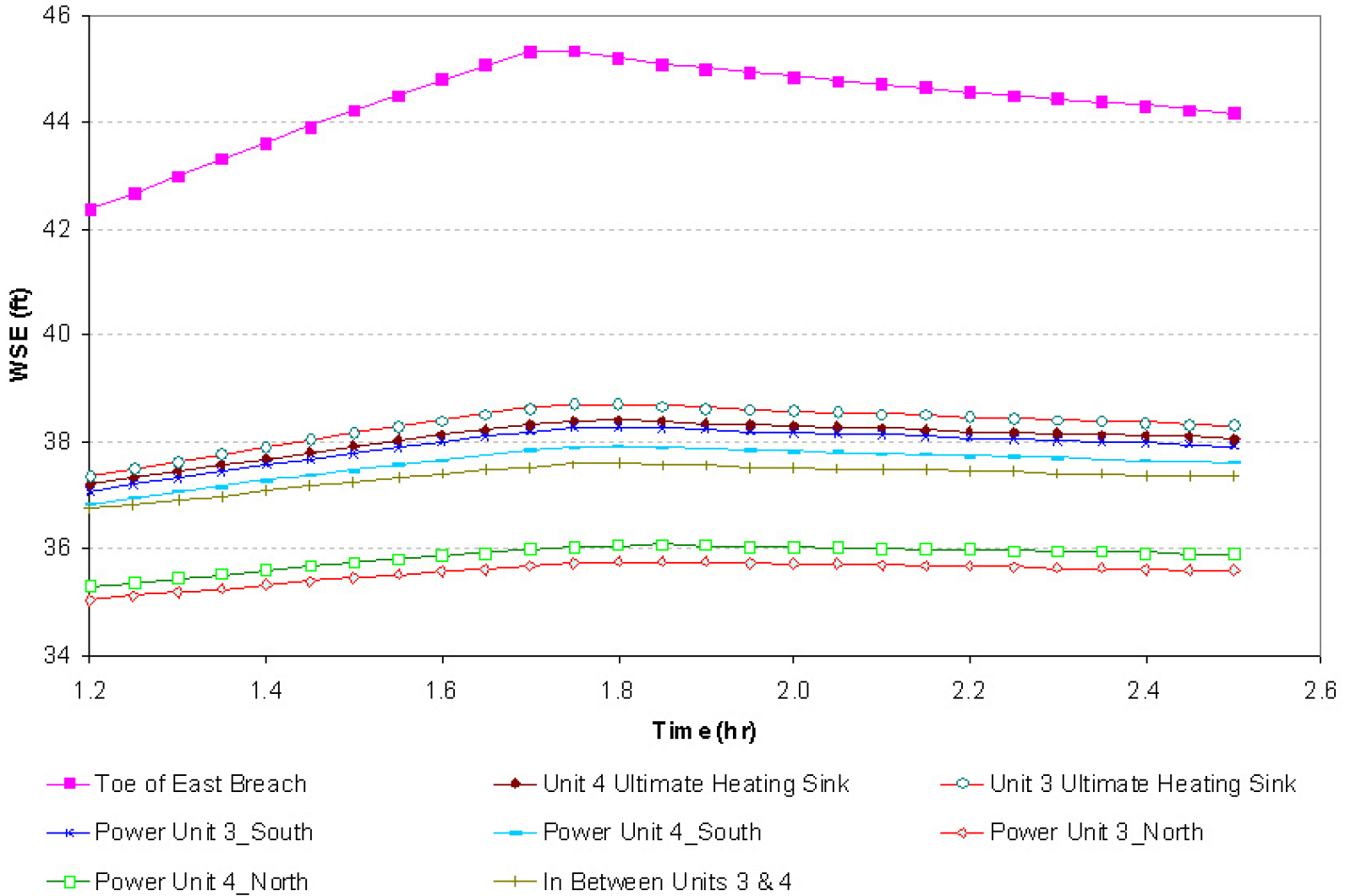
Figure 2.4S.4-20 Time-Dependent Water Surface Elevations Associated with East Breach Scenario
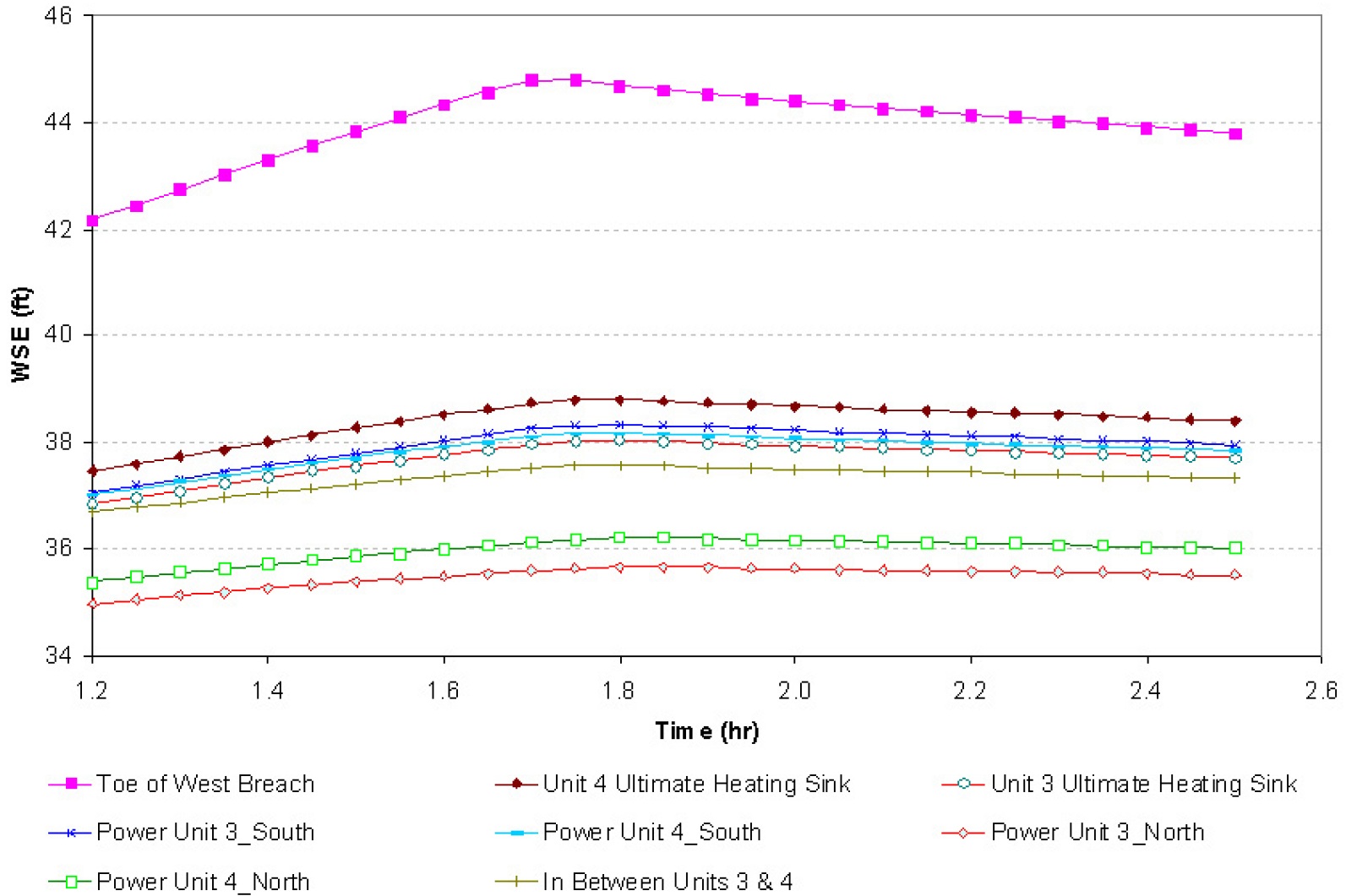
Figure 2.4S.4-21 Time-Dependent Water Surface Elevations Associated with West Breach Scenario
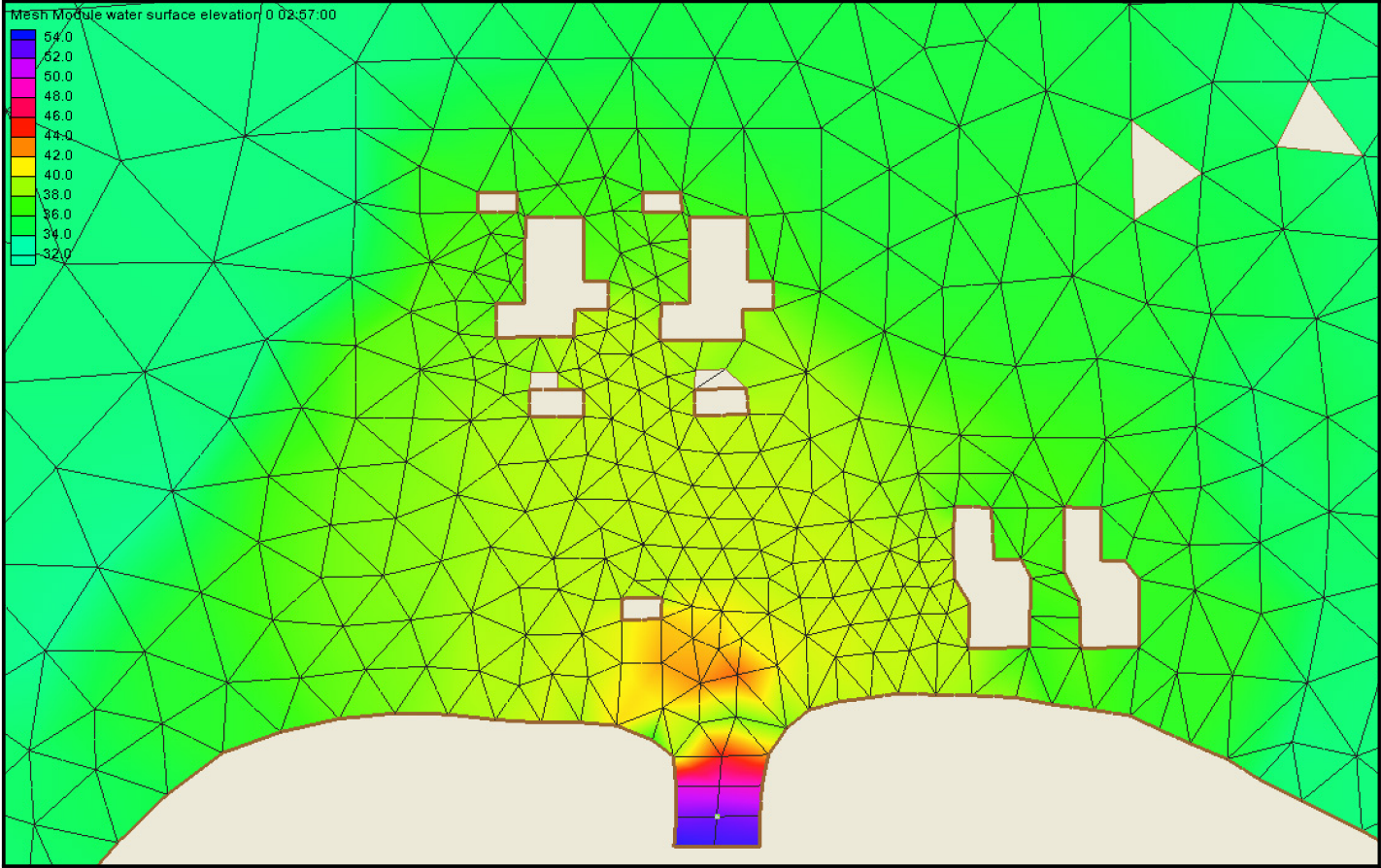
Figure 2.4S.4-21a Peak Water Surface Elevations Associated with East Breach Scenario (at time = 1.75 hours after initiation of breach)
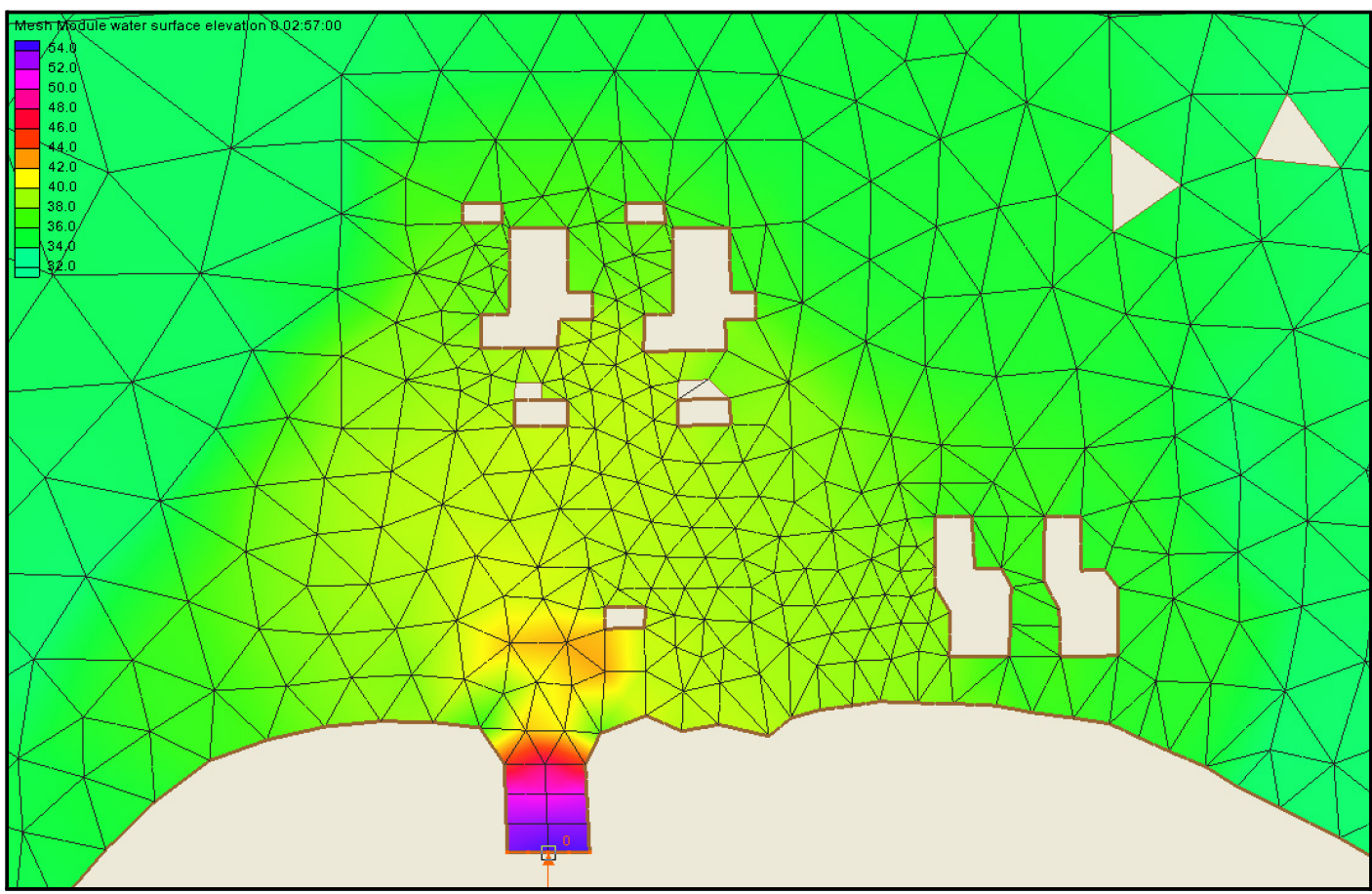
Figure 2.4S.4-21b Peak Water Surface Elevations Associated with West Breach Scenario (at time = 1.75 hours after initiation of breach)
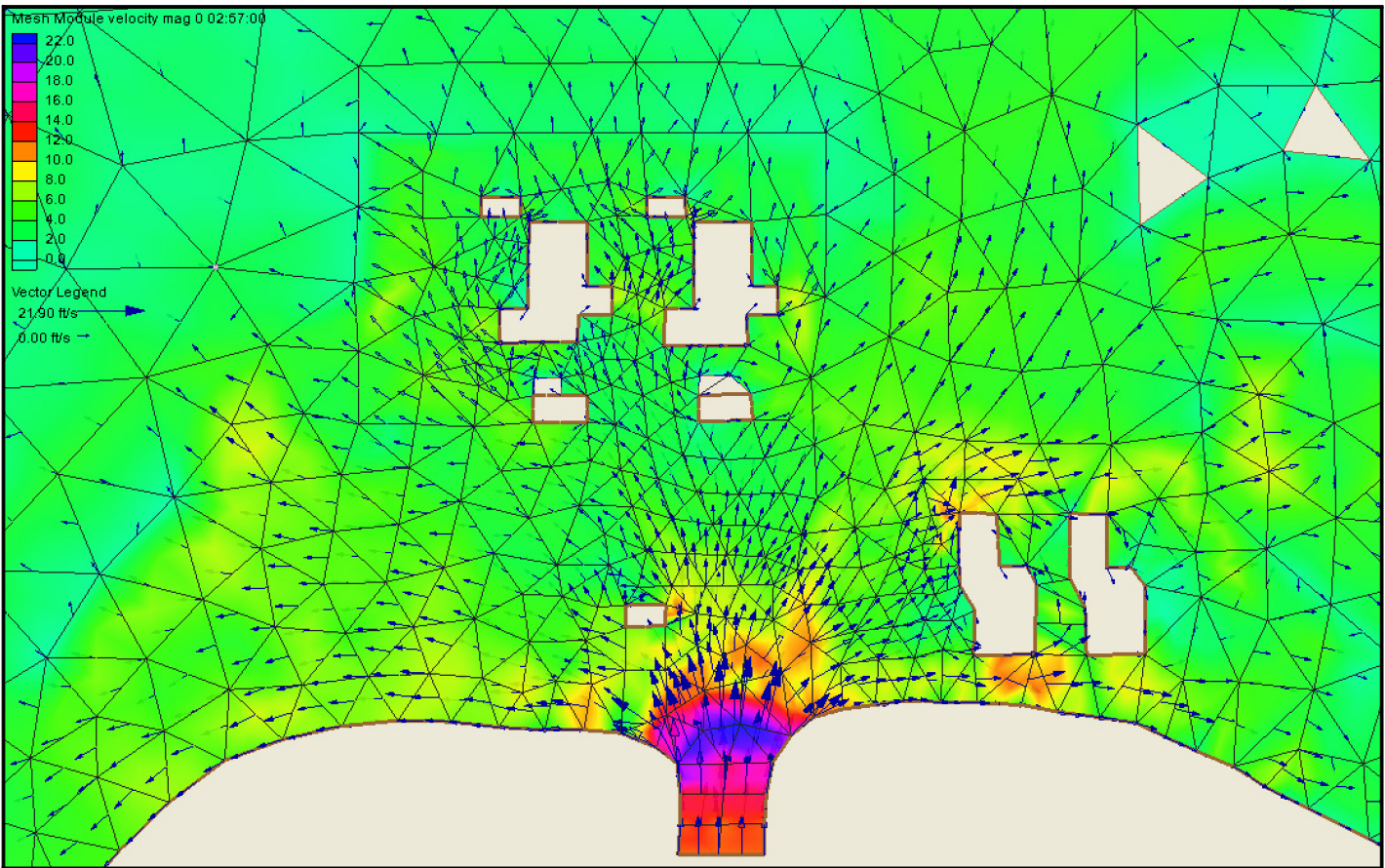
Figure 2.4S.4-21c Peak Velocities Associated with East Breach Scenario (at time = 1.75 hours after initiation of breach)
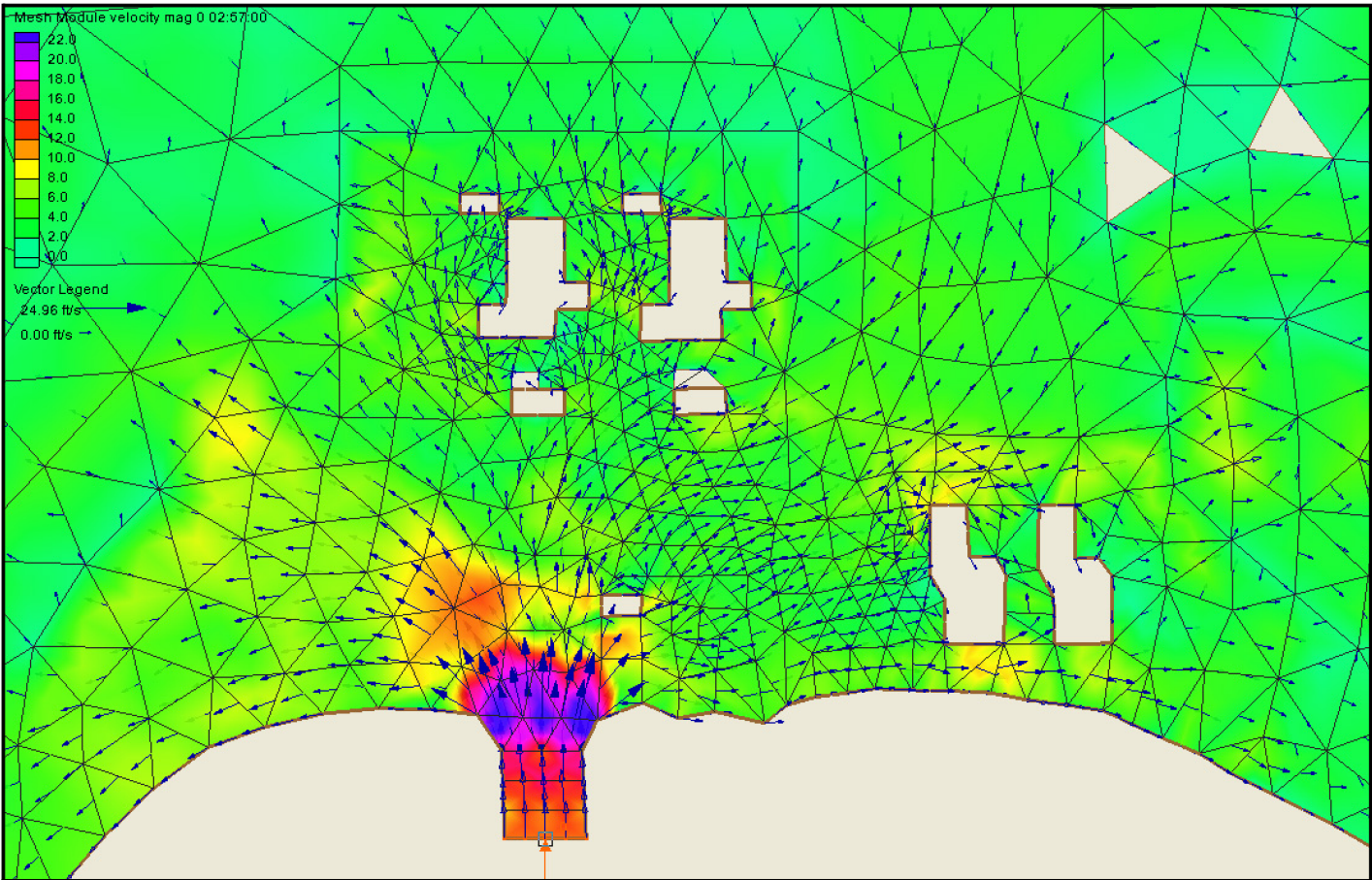
Figure 2.4S.4-21d Peak Velocities Associated with West Breach Scenario (at time = 1.75 hours after initiation of breach)
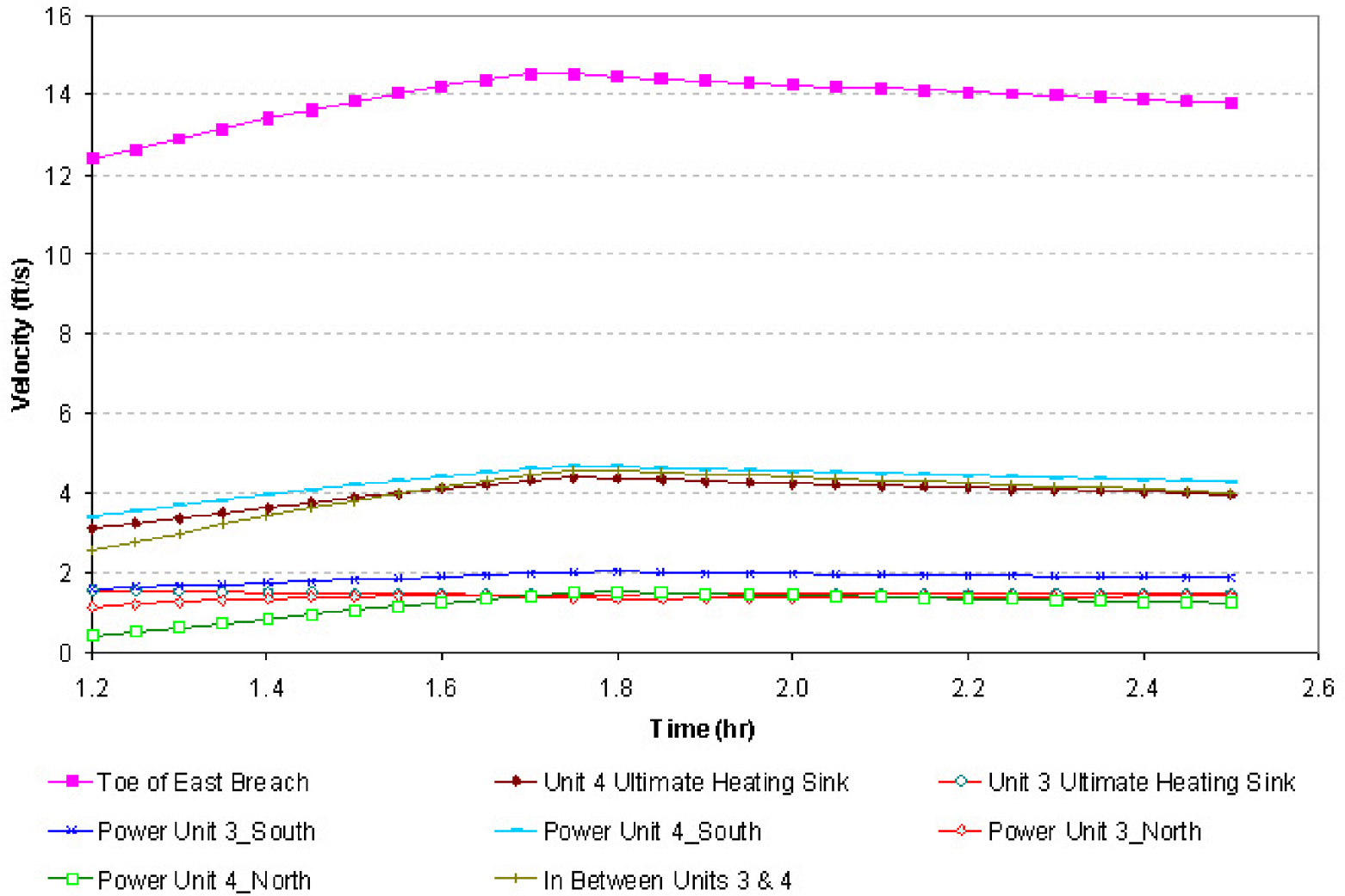
Figure 2.4S.4-21e   Time-Dependent Velocities Associated with East Breach Scenario
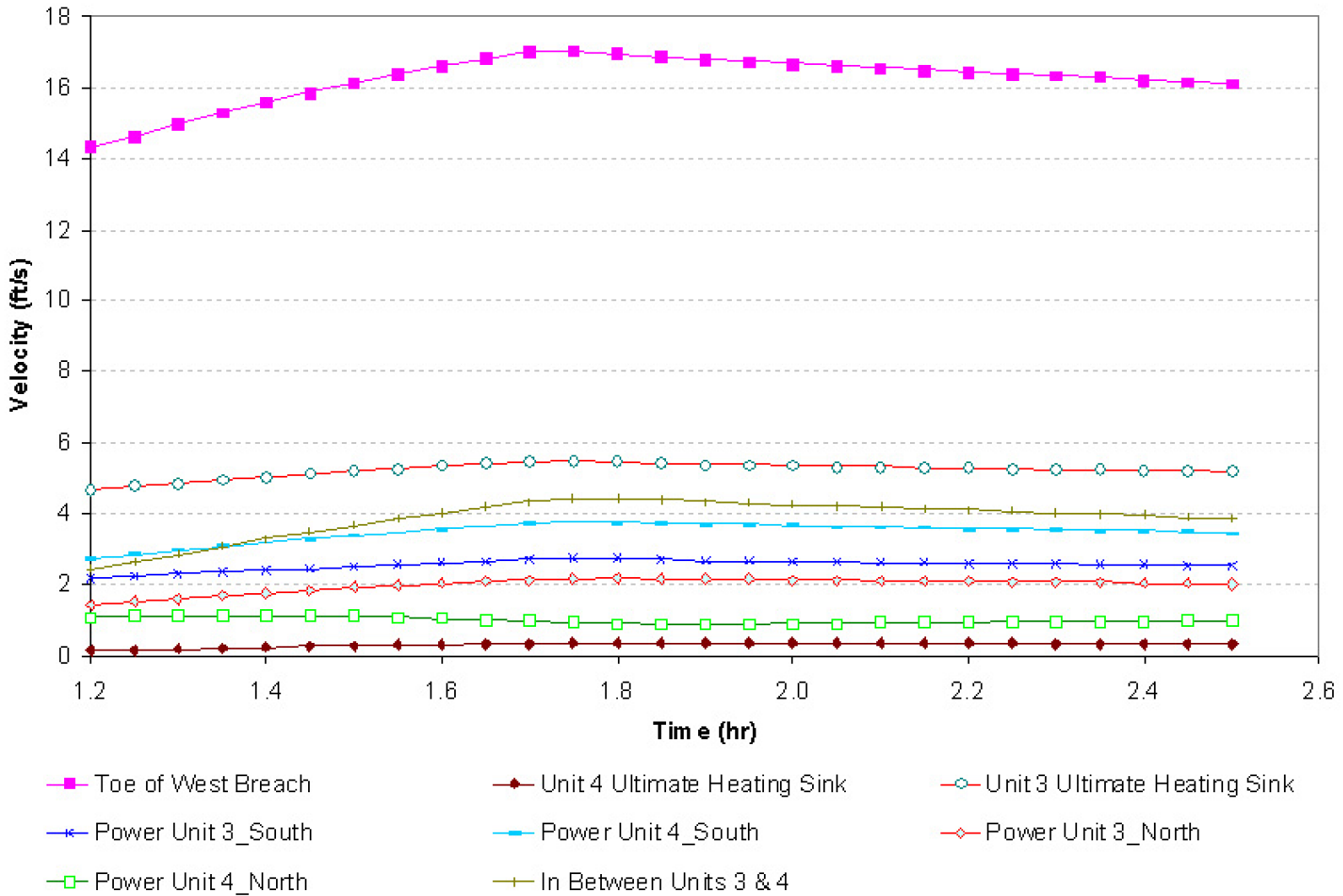
Figure 2.4S.4-21f Time-Dependent Velocities Associated with West Breach Scenario
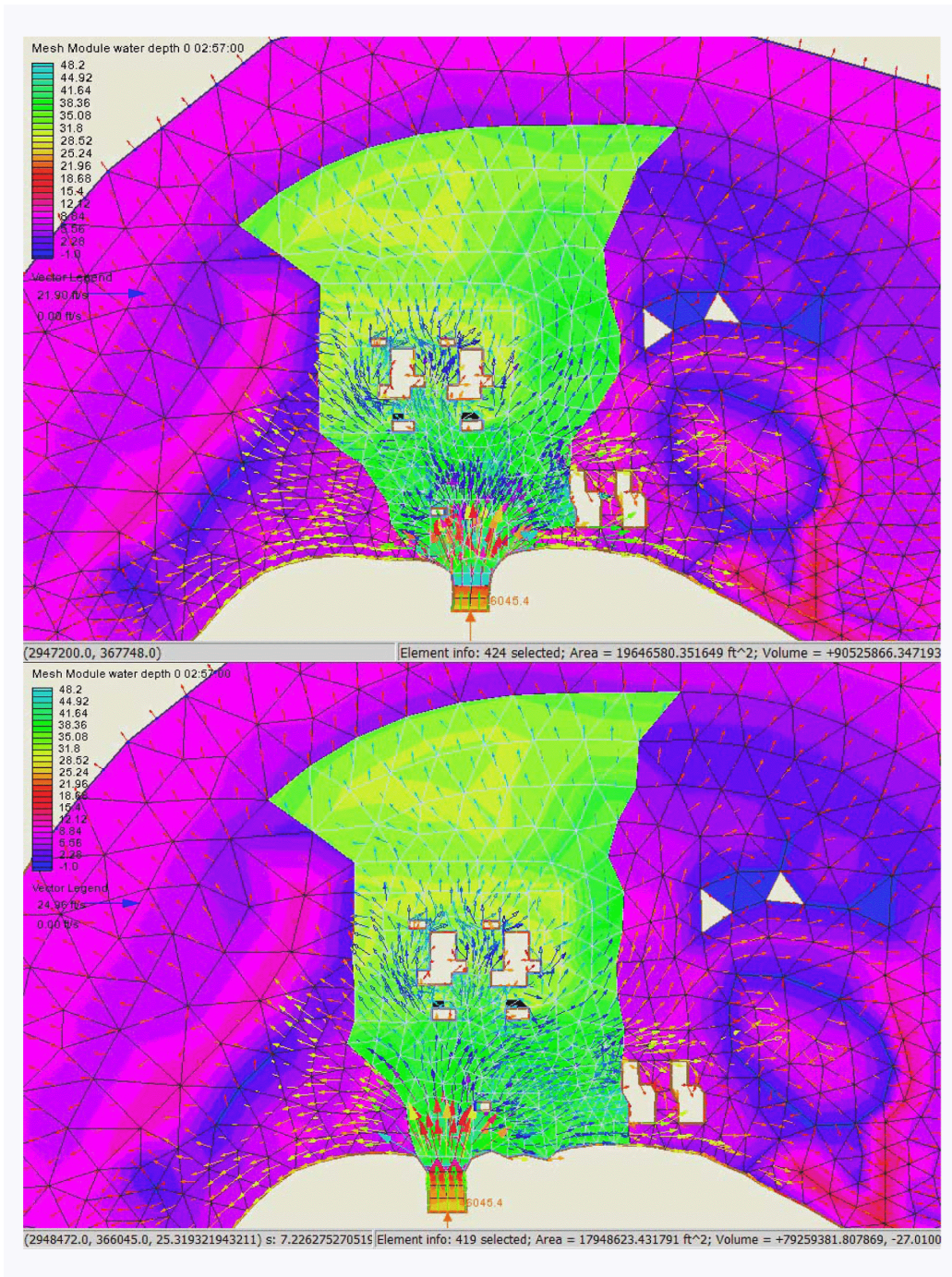
Figure 2.4S.4-21f1 Selected Fan Areas Associated with East Breach Scenario (top) and West Breach Scenario (bottom)
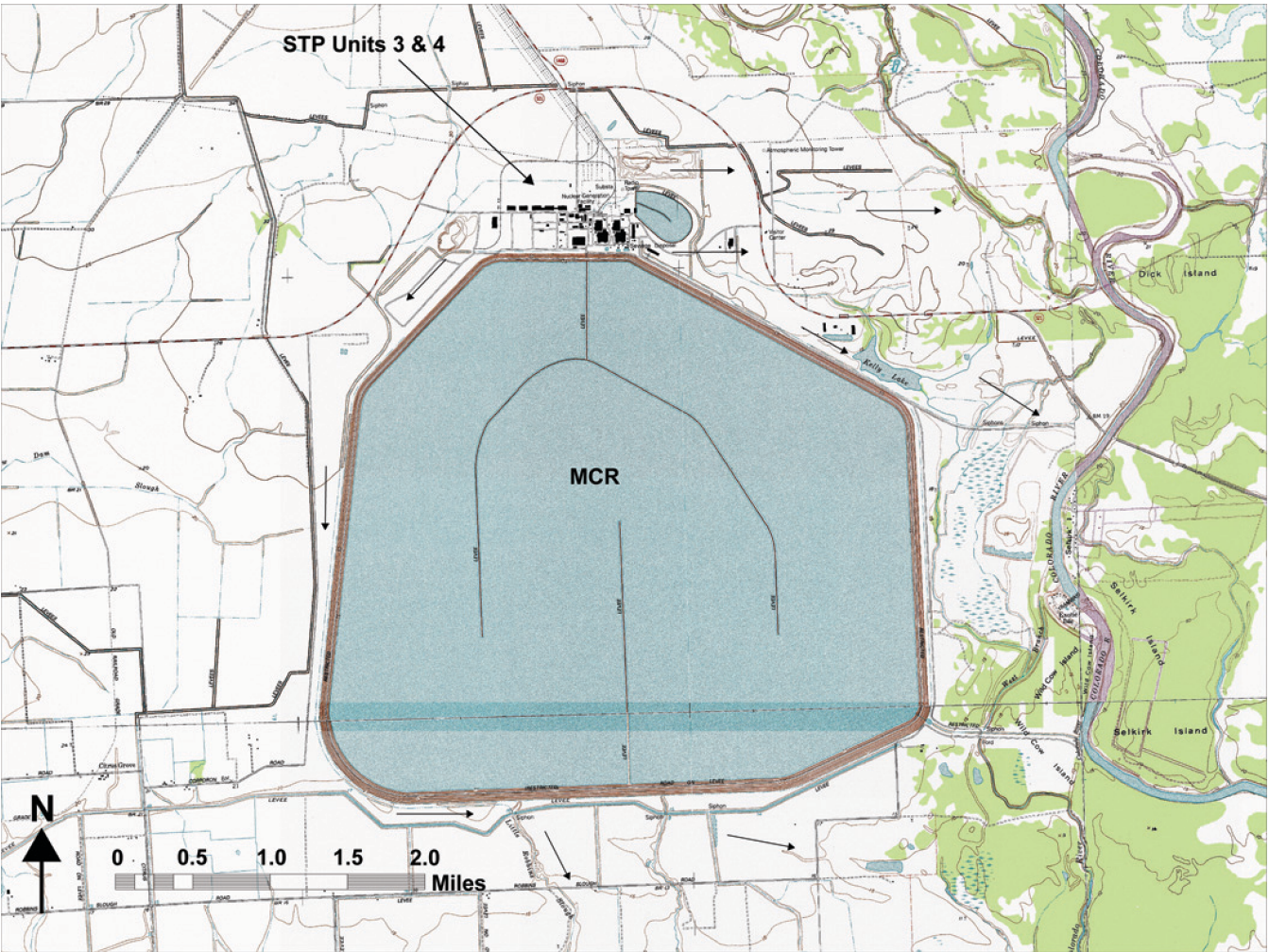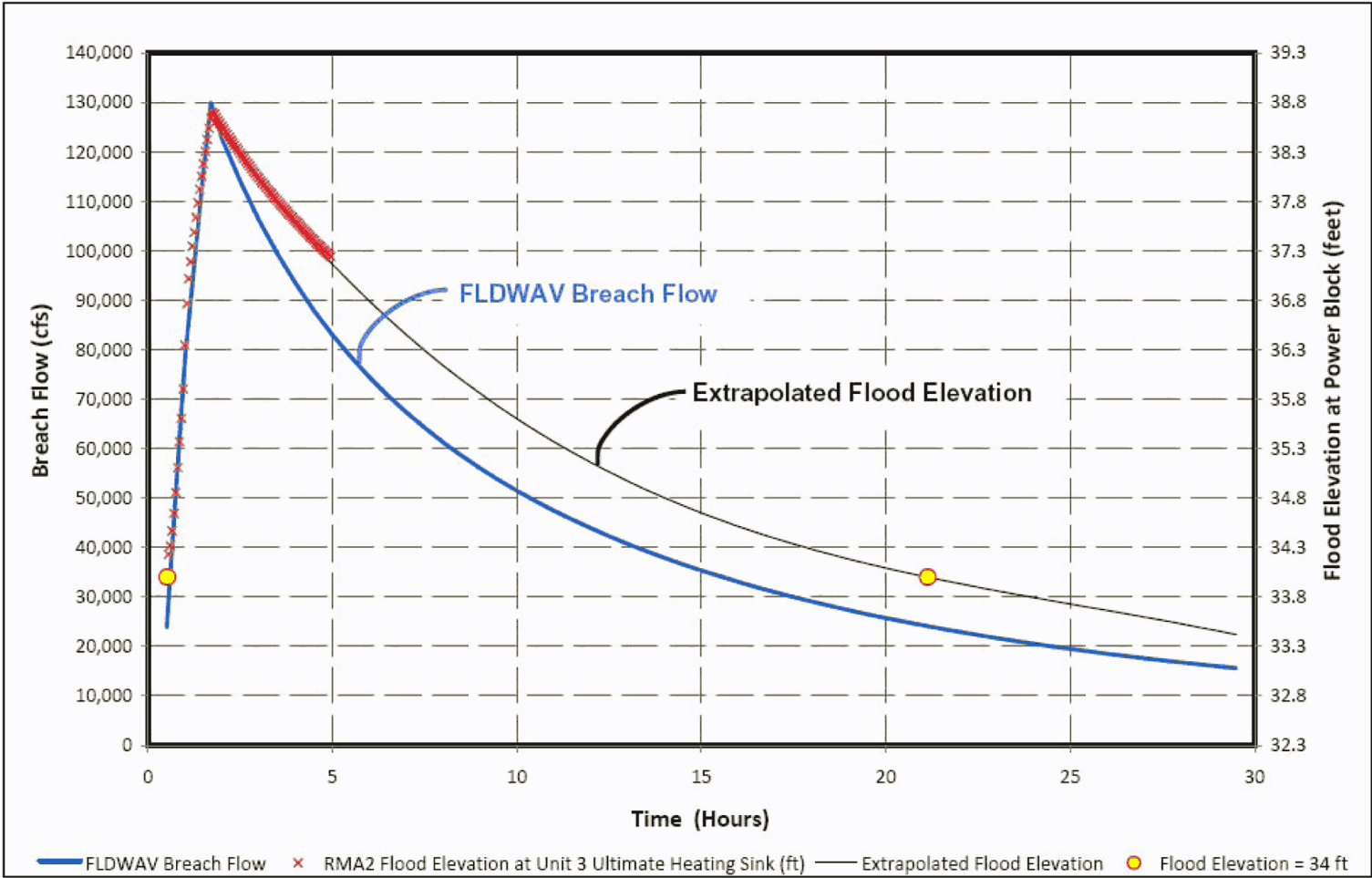
Figure 2.4S.4-21i Stream System around STP Site

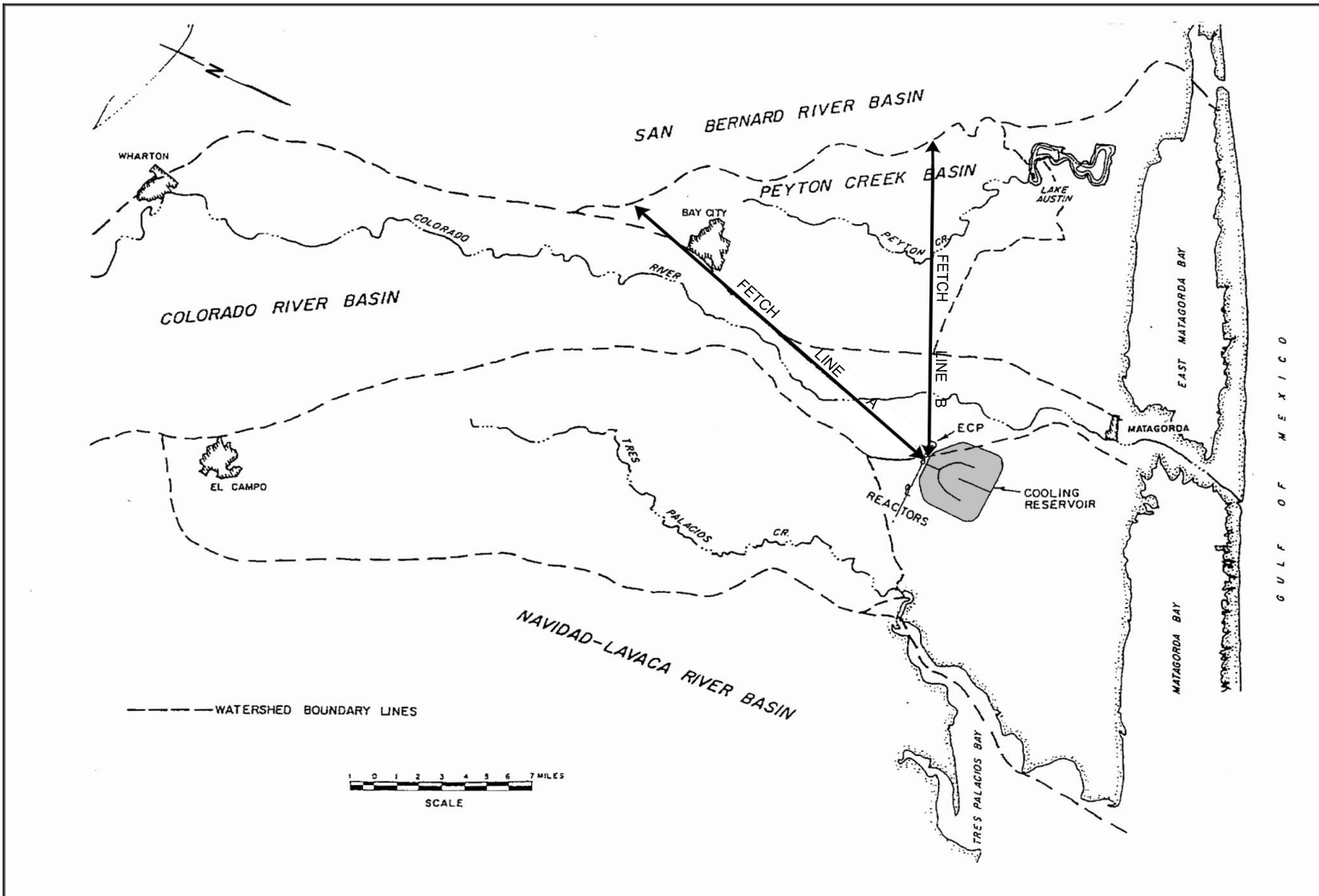**Figure 2.4S.4-21j Breach Outflow and Flood Elevation to Determine Duration of Inundation at Safety-Related SSCs**

Figure 2.4S.4-22 Fetch Directions and Length